coatings

MDPI

Article

Rheological Properties and Microstructure of Waterborne Epoxy Resin Modified Emulsified Asphalt

Wei Zhang [1], Shi Hu [1], Shuai Zhang [1], Qin Liu [1], Yihan Shi [2] and Jian Ouyang [3,*]

[1] Zhejiang Communications Investment Group Construction Management Co., Ltd., Xiaoshan District, Hangzhou 311200, China
[2] School of Transportation and Logistics, Dalian University of Technology (Lingshui Campus), Linggong Road, Dalian 116024, China
[3] State Key Laboratory of Tropic Ocean Engineering Materials and Materials Evaluation, School of Civil Engineering and Architecture, Hainan University (Haidian Campus), Meilan District, Haikou 570228, China
* Correspondence: ouyangjian@hainanu.edu.cn

Abstract

As a road repair material, emulsified asphalt offers advantages such as convenient construction, good fluidity, and environmental safety. However, its relatively low strength limits its application range, making performance enhancement a key research focus. In this study, waterborne epoxy resin (WER) was used to modify emulsified asphalt, and the preparation process and performance were systematically investigated. Three types of waterborne epoxy systems were selected, and through compatibility, film-forming performance, and bonding strength tests, the JT waterborne epoxy system was identified as having the best overall performance, with an optimal epoxy-to-curing-agent ratio of 1:0.6. Modified emulsified asphalts with different proportions of WER and styrene–butadiene rubber were prepared. Using fluorescence microscopy, image recognition techniques, and multiple experimental evaluations, the distribution of epoxy resin in the emulsified asphalt was quantitatively analyzed. The results show that the addition of WER significantly improves the bonding strength of emulsified asphalt, with the fastest rate of increase observed in the 5−10% range. However, a comprehensive evaluation considering microstructure uniformity, rheological performance, and water resistance indicates that the optimal overall performance is achieved in the 10−12% range, and the WER content should strictly be controlled below 15% to avoid severe local agglomeration. Meanwhile, the modified water-boiling test reveals that the adhesion between WERAE and aggregates is significantly enhanced, implying a potentially improved resistance to moisture-induced damage under practical service conditions. The standard deviation of area results indicate that when the WER content exceeds 15%, local agglomeration occurs, which is unfavorable for strength development of the modified system; the distribution uniformity results further show that when the WER content is greater than 12%, it negatively affects the uniform dispersion of WER within the emulsified asphalt.

Keywords: emulsified asphalt; waterborne epoxy resin; modification; bonding strength; water resistance; dispersion

Check for updates

Academic Editor: Eduardo Guzmán

Received: 8 July 2026
Revised: 6 August 2026
Accepted: 12 August 2026
Published: 15 August 2026

Copyright: © 2026 by the authors. Licensee MDPI, Basel, Switzerland. This article is an open access article distributed under the terms and conditions of the Creative Commons Attribution (CC BY) license.

1. Introduction

The rapid expansion of infrastructure has increased the demand for maintenance and rehabilitation and raised the performance requirements for maintenance materials. Emulsified asphalt, with advantages such as convenient construction, good fluidity, and

the ability to be applied at relatively low temperatures, can effectively reduce energy consumption and harmful emissions during road construction, meeting the requirements of green construction and environmental protection [1,2]. It has therefore been widely used in highway maintenance and cold-mix applications. However, despite these advantages, emulsified asphalt still has certain limitations. First, compared with conventional base asphalt, it generally exhibits lower strength, which restricts its application in pavement projects with strict strength requirements. Second, its relatively low durability and reliability can increase maintenance frequency, thereby raising long-term maintenance costs. Based on these limitations, research on modified emulsified asphalt has become an important direction for improving pavement material performance.

Waterborne epoxy resin-modified emulsified asphalt (WERAE), as a high-performance modified material in road engineering, has been studied since 2008. Zhang et al. improved the performance of emulsified asphalt in clay coatings by incorporating 3% styrene–butadiene rubber (SBR) latex and 3% waterborne epoxy resin (WER), significantly enhancing its high- and low-temperature performance, shear strength, and storage stability [3]. In terms of material system design, Liu applied a response surface methodology (RSM) model for multi-factor and multi-response optimization, considering the ratio of waterborne epoxy resin to emulsified asphalt, polymer content, defoamer content, and mixing speed, providing insights for the design of toughness-enhanced semi-flexible pavement materials [4]. Yang used a two-component waterborne epoxy resin to modify neat emulsified asphalt, showing improved binder performance and enhanced pothole repair performance, and recommended a WER content range of 15–20% for repair materials [5]. Yang further focused on interfacial bonding in pothole repair and developed waterborne epoxy–SBR-modified emulsified asphalt (SW), which exhibited excellent shear and tensile strength under various environmental conditions [6]. Li et al. confirmed through evaporation tests that an appropriate amount of WER can simultaneously improve the high- and low-temperature performance and mechanical properties of asphalt mixtures [7].

With respect to performance evaluation, WER imparts thermosetting characteristics to emulsified asphalt, extending beyond the scope of traditional asphalt evaluation systems. Existing studies mainly focus on mechanical indices such as bonding strength and shear strength, but issues remain, including inconsistent test methods and specimen specifications, lack of unified evaluation standards, and limited general applicability of conclusions. Rheological properties, which can comprehensively reflect high-temperature stability, low-temperature cracking resistance, and fatigue resistance, have become a key direction for standardized evaluation of WERAE. Feng et al. reported that epoxy resin-SBS-T composite modifiers significantly improve high-temperature performance, with notable enhancement when the content exceeds 6% [8]. He demonstrated through dynamic shear rheometer (DSR) tests that WER forms a cross-linked network structure in emulsified asphalt, significantly enhancing high-temperature stability and fatigue resistance [9]. Li applied Fourier transform infrared spectroscopy (FTIR) to characterize oxidation reactions in pressure-aging vessel (PAV) tests and evaluated rheological behavior before and after aging using DSR, showing that WER improves resistance to oxidative aging [10]. Yang et al. found that SW binders exhibit better aging resistance [11], while Yang et al. identified 3% as the optimal WER content for WESAE, with excessive content adversely affecting storage stability and particle distribution uniformity. Huang et al. observed that when WER content is below 15%, it exists as a continuous phase, improving aggregate–asphalt cohesion and rutting resistance [12].

The micro-mechanism is central to understanding the performance enhancement of WERAE. In recent years, techniques such as X-ray Diffraction (XRD), Scanning Electron Microscopy (SEM), and FTIR have enabled deeper insights into structural evolution and

interfacial behavior [13]. Cong et al. characterized EA binders in terms of viscosity, tensile strength, elongation at break, compatibility, morphology, glass transition temperature (Tg), contact angle, and surface free energy, showing that curing temperature and asphalt content significantly affect properties [14]. Han combined performance tests and SEM analysis to show that emulsions and curing agents polymerize within the emulsified asphalt medium to form epoxy resin, with modification mainly governed by physical effects; when WER exceeds 12%, a continuous network structure forms [15]. Li used molecular dynamics simulations to model the interface between WEREA and aggregates, indicating stronger adhesion to alkaline aggregates than to acidic ones [16]. Ji found that epoxy emulsions optimize pore structure, with optimal mechanical and toughness performance at 30% content [17]. Gu et al. identified chemical incompatibility in WER–emulsified asphalt–rubber powder systems, requiring careful control [18]. Cuadri et al. revealed through FTIR and SARA analysis that esterification and etherification reactions occur between epoxy resin and aromatic/resin components in asphalt, forming high-molecular-weight compounds that enhance performance [19]. Wang et al. found that 10% WER provides the best dispersion, improving softening point, reducing permeability, and enhancing high-temperature and bonding properties [20]. Ji et al. observed that WER addition transforms the phase structure into a three-dimensional interpenetrating network, significantly increasing viscosity and tensile strength [21].

Furthermore, it should be noted that the surface free energy of the asphalt binder is crucial for quantifying the adhesive bond between asphalt and aggregate. When the asphalt binder is incorporated into an asphalt mixture, the interaction between the filler and the binder significantly affects the stiffness, fatigue resistance, and moisture susceptibility of the resulting mastic and mixture [22]. In the context of WERAE, the introduction of filler may further affect the dispersion of the epoxy phase and the formation of the thermosetting network. Although the present study focuses primarily on the binder-level evaluation and microstructural quantification of WERAE without filler, this factor is of crucial importance. Future investigations will incorporate the effect of mineral filler to bridge the gap between binder performance and mixture behavior.

The main deficiencies of existing research lie in the following aspects: in terms of mix design, a systematic screening of WERs that are widely available, cost effective, and highly compatible with emulsified asphalt is lacking; in terms of performance evaluation, the thermosetting nature renders conventional indicators invalid, and an applicable evaluation system has yet to be established; and in terms of microstructural analysis, techniques such as fluorescence microscopy remain limited to qualitative observation with strong subjectivity, and quantitative indicators are lacking to objectively characterize the local agglomeration and global dispersion of WER.

This study addressed three key questions: screening a practical WER system, establishing a performance evaluation method for thermosetting WERAE, and quantitatively characterizing WER dispersion while correlating it with macroscopic properties. It was hypothesized that dispersion uniformity governs modification effectiveness, that WER and SBR act synergistically, and that an optimal dosage range exists where microscopic and macroscopic performance are simultaneously optimized. Through macro–micro coupled evaluation, the JT system was identified; an image analysis algorithm combining block-wise adaptive histogram equalization with local dynamic thresholding was developed, and two quantitative indicators, area standard deviation and distribution uniformity standard deviation, were proposed. The synergistic mechanism was revealed, and the optimal dosage range of 8–12% was determined, thereby providing a theoretical basis for formulation design.

2. Materials and Testing

2.1. Materials

The waterborne epoxy curing system consists of a WER and a waterborne curing agent. The epoxy resin itself is not soluble in water, but it can be dispersed in water through specific processing techniques, which also helps reduce its brittleness [23]. Uncured epoxy resin is a thermoplastic oligomer with low strength when used alone; only after the addition of a curing agent and the formation of a crosslinked network can it exhibit superior performance. Given the wide variety of epoxy resins and curing agents, selection is critical for the development of WERAE.

WERs are widely used in the coatings field [24–26], and their evaluation indices are primarily derived from film and coating standards, with limited guidance available in road engineering specifications. In this study, coating-related standards are referenced, with particular attention to the performance after blending with emulsified asphalt. The compatibility between WER and emulsified asphalt is comprehensively evaluated based on curing rate, film-forming quality, intrinsic strength, compatibility, and dissolution rate.

2.1.1. Material Selection

A 90# base asphalt sourced from Petro China (Beijing, China) was used as the raw material for preparing the emulsified asphalt. To identify a suitable waterborne epoxy system, three commercially available systems were selected and subjected to performance evaluation. The three WER systems—HM, JT, and KST—were supplied by Heima Chemical, Lingwei Technology, and Shenyang Baichen Chemical Technology Co., Ltd (Changzhou, Hangzhou, Shenyang, China), respectively. The relevant properties of the base asphalt, emulsifier, and the three waterborne epoxy systems are summarized in Tables 1–5. All component dosages in the table are based on external addition, i.e., by mass of the emulsified asphalt; the epoxy resin and curing agent were prepared at a mass ratio of 1:0.6.

Table 1. Properties of the waterborne epoxy resins.

Type	Appearance	Solid Content (%)	Epoxy Equivalent (g/eq)	Viscosity (mPa·s)	pH
HM (BH-653)	Milky white viscous liquid	60 ± 2	180–230	1000–2000	6–7
JT (JT-WBE522)	Milky white resin emulsion	50 ± 3	400–800	<1000	2–5
KST (K-051)	Milky white liquid	50 ± 2	360–380	6500 ± 500	6.5–7.5

Table 2. Properties of the waterborne curing agents.

Type	Appearance	Solid Content (%)	Active Hydrogen Equivalent (g/eq)	Viscosity (mPa·s)	pH
HM (BH-532)	Light yellow homogeneous fluid	40 ± 2	170–190	1000	9–10
JT (JT-WBH817)	Light yellow homogeneous fluid	44 ± 2	200–320	>2000	8–11
KST (K-17)	Light yellow transparent liquid	90 ± 2	190–200	6500 ± 500	10–13

Table 3. Main technical properties of the asphalt.

Property	Measured Value	Specification
Penetration (25 °C, 0.1 mm)	92	90–100
Softening Point (°C)	45	>40
Ductility (15 °C, cm)	>100	>100
Wax content (%)	1.2	<2.2

Table 4. Technical specifications of the emulsifier.

Property	Value
Dosage (%)	3
Appearance	Brownish-red liquid
Active content (%)	>37
pH	2–9

Table 5. WERAE experimental formulations.

Mix ID	WER Content	SBR Content
A-1	0%	0%
A-2	5%	0%
A-3	8%	0%
A-4	10%	0%
A-5	12%	0%
A-6	15%	0%
A-7	20%	0%
B-1	5%	3%
B-2	8%	3%
B-3	10%	3%
B-4	12%	3%
B-5	15%	3%
B-6	20%	3%

2.1.2. Emulsified Asphalt

The procedure for preparing the emulsified asphalt is as follows. The base asphalt was heated in an oven at 135 °C until completely molten. An emulsifier was mixed with water at a dosage of 3%, and the pH of the mixture was adjusted to approximately 2 using hydrochloric acid, while the temperature of the soap solution was maintained at 55 °C. The molten asphalt and the soap solution were then combined at a mass ratio of 60:40, poured into a colloid mill, and sheared at 140 °C for 2 min to obtain a high-quality emulsified asphalt. The preparation process is illustrated in Figure 1.

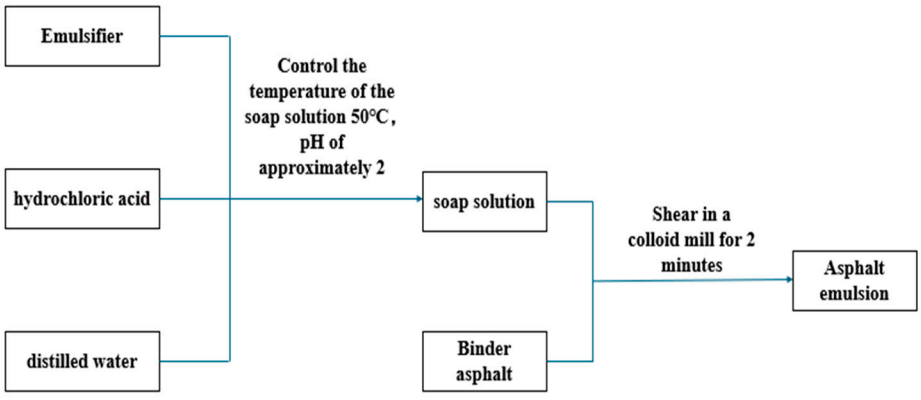


Figure 1. Process of preparing the emulsified asphalt.

2.1.3. WERAE

During the preparation process, the curing agent was first added to the emulsified asphalt and uniformly mixed using a mechanical stirrer at 500 rpm for 5 min at room temperature (approximately 25 °C). Subsequently, the WER was added and stirred under the same conditions for 5 min to ensure thorough dispersion. After the WERAE was prepared, SBR latex (Liangning Lutong Group, solid content 60%) was added. To avoid

making hasty choices regarding the dosage, this study first conducted a pretest to examine the modification effect of SBR latex within the range of 2% to 4%. After comprehensive comparison, 3% was selected as the optimal dosage, and based on this, a systematic analysis of the performance of WERAE was carried out. Previous studies indicate that the WER content in WERAE typically ranges from 5% to 30% [5,6]. Considering practical application and cost, four WERAE formulations with epoxy resin contents of 5%, 10%, 15%, and 20% were prepared in this study, with a fixed resin-to-curing-agent ratio of 1:0.6.

The basic gradient levels of 5%, 10%, 15%, and 20% were selected, and 8% and 12% were further introduced based on the following preliminary compatibility test findings: a WER content of around 8% represents the critical point at which the epoxy particles begin to form the embryonic spatial network; the range between 12% and 15% constitutes the key threshold interval within which the microstructure transitions from uniform dispersion to local agglomeration. Refining the sample preparation within this interval is therefore crucial for exploring the correlation between microscopic uniformity and macroscopic mechanical properties.

2.2. Testing

2.2.1. Performance Tests of Waterborne Epoxy Systems

Compatibility Test

During the development and optimization of WERAE, ensuring good compatibility between the two materials is essential. Good compatibility not only affects the uniformity and stability of the final product, preventing segregation and agglomeration during preparation, but also directly determines its workability and durability in pavement construction. To evaluate the water solubility of the curing agent, a miscibility test with water was conducted. The curing agent was mixed with water at mass ratios of 1:1, 1:3, and 1:5. The dissolution rate was observed, and the mixtures were left to stand for one day to assess whether phase separation occurred.

Particle Size Distribution Test

The compatibility between WER and emulsified asphalt is commonly evaluated by measuring the particle size distribution of their mixtures. Laser diffraction particle size analysis is a widely used and effective method for this purpose. In this study, an LS-POP(9) laser particle size analyzer (Zhuhai Aomeike Instrument Co., Ltd., Zhuhai, China) was employed, as shown in Figure 2. The instrument operates based on the physical principle of light scattering, determining particle size distribution by measuring the scattering angle and intensity of a laser beam passing through the sample. The scattering angle is inversely related to particle size, allowing the particle size distribution to be accurately characterized.

The specific operational parameters for the laser diffraction measurements were set as follows: deionized water was used as the dispersion medium; the samples were ultrasonicated at a power of 40 W for 2 min and immediately tested to minimize re-agglomeration; the refractive index was set to 1.65 for the analyte (asphalt/epoxy) and 1.33 for the dispersion medium; the obscuration was controlled within the range of 10% to 15%; measurements were conducted under the general measurement mode. For each sample formulation, the particle size distribution was measured three times, and the average value was recorded to ensure data reliability.

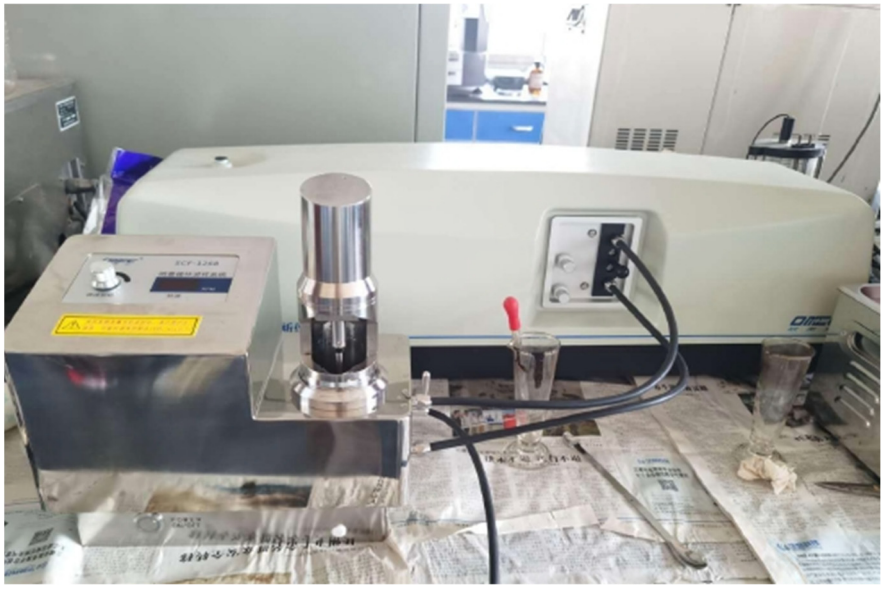


Figure 2. LS-POP (9) laser particle size analyzer.

Film-Forming Performance Test

The film-forming performance test can reflect the reaction rate and reaction uniformity of the waterborne epoxy system. Through this test, both the surface drying time and the hard drying time of the system can be determined. The surface drying time is defined as the time when the coating film becomes tack-free to the touch, where a finger lightly touches the surface and feels slightly sticky but does not adhere. The hard drying time is defined as the time when a piece of qualitative filter paper is placed on the coating surface, and after applying a drying tester and rotating it, the filter paper can freely fall off, indicating complete drying.

2.2.2. WERAE Tests

Evaporation Residue

Based on relevant literature, the evaporation residue of WERAE was prepared using a room-temperature evaporation method, which can be used for preparing specimens for rheological tests [27]. Specifically, the prepared WERAE was poured into a silicone mold. Since rheological testing requires specimens with a thickness of 1 mm, while emulsified asphalt contains a large amount of water, the casting thickness in the mold was controlled at 2 mm. The samples were then allowed to evaporate at room temperature. After three days, demolding was performed to obtain asphalt sheets with the desired thickness, which were subsequently cut into appropriate sizes for testing.

DSR Test

For bonding strength, DSR rheological, and particle size tests, 3 parallel specimens (n = 3) were tested for each formulation. The DSR is an experimental device used to assess the viscoelastic properties of materials. It is also a standard testing method for determining the high- and low-temperature PG values of asphalt binders [28,29], and is widely applied in the performance evaluation of asphalt and its modified products. The testing system consisted of an air-compression unit, the rheometer, and a computer control system. A parallel plate with a diameter of 25 mm was selected, and the sample thickness was set to 1 mm. For the temperature sweep test, the frequency was fixed at 10 rad/s, and measurements were conducted from 46 °C to 70 °C, with a temperature increment of 6 °C [30]. The frequency sweep test was performed over the same temperature range,

with the frequency varying from 0 to 100 rad/s. The tested samples included evaporation residues of emulsified asphalt modified with 5%, 8%, 10%, 12%, and 15% WER, as well as residues of emulsified asphalt modified with corresponding WER contents combined with 3% SBR. Prior to testing, strain sweep and frequency sweep tests were conducted to ensure that all measurements were performed within the linear viscoelastic region.

2.2.3. Microstructure and Surface Characterization Tests

Fluorescence Microscopy Test

For fluorescence microscopy image analysis, 5 distinct fields of view (n = 5) were randomly selected for statistical processing for each WER content sample. Epoxy resin, as a special organic molecule, can emit yellow-green fluorescence under blue light excitation, whereas asphalt and SBR latex do not exhibit fluorescence under the same wavelength. This characteristic enables fluorescence microscopy to be used to observe the fluorescence behavior of WERAE with different epoxy resin contents. To ensure the accuracy of the observations, the prepared sample sections must maintain a certain thickness and be free of air bubbles. In this study, a fluorescence microscope manufactured by Olympus Corporation (Tokyo, Japan) was used, as shown in Figure 3. The magnification was set to 400, and the fluorescence distribution of WERAE under different epoxy resin dosages was recorded. The sample preparation procedure is as follows: a drop of WERAE was first taken using a glass rod and then gently covered with a coverslip. The specimen was left to cure for 24 h before observation. The prepared samples are shown in Figure 4.

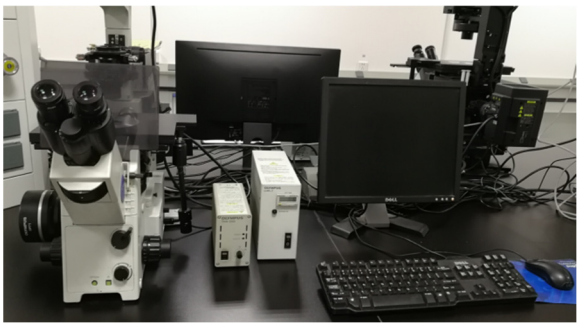


Figure 3. Fluorescence microscope.

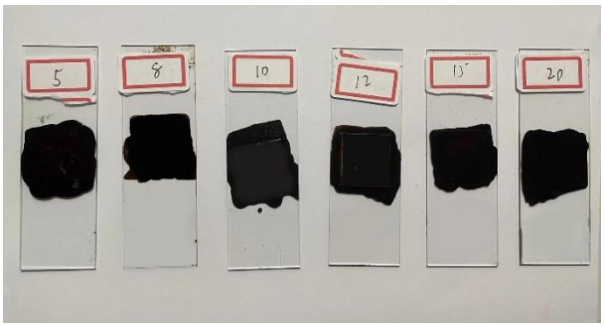


Figure 4. Fluorescence microscopy test samples.

Image Analysis

Based on the characteristics of the fluorescence microscopy images, one image recognition algorithm was adopted to process the fluorescence micrographs. The algorithm was manually designed to capture the distribution of epoxy resin in the asphalt by utilizing the fluorescence intensity of bright spots, which effectively reflects key image features.

(1) Implementation procedure

In fluorescence image processing and analysis, binarization is the most critical step. It simplifies complex images by highlighting the epoxy resin structure in white against a black background, thereby enhancing contrast.

The algorithm consists of the following steps:

Preprocessing: The original images were first converted from color to grayscale to simplify the information and emphasize the intensity differences. Noise reduction filtering and contrast adjustment were then applied to enhance the relevant features while suppressing irrelevant information, thereby improving overall image quality.

Image binarization: Based on the preprocessed images, an adaptive threshold segmentation method was used for binarization. This method dynamically adjusts the threshold according to local brightness variations, making it suitable for fluorescence images with complex illumination conditions. It enables accurate separation of fluorescent regions from the background, allowing for precise detection of fluorescent spots.

Result visualization: After binarization, the detected fluorescent regions were overlaid on the original images for visualization, facilitating further analysis and data processing.

Through the above procedure, the epoxy resin structures labeled by fluorescence were accurately extracted from the original images.

(2) Algorithm design and optimization

Initial algorithm selection: For images with relatively distinct features, mature adaptive thresholding methods are commonly used for binarization. Among various algorithms, Otsu's method and the Triangle method perform well in preliminary processing. Otsu's method is an adaptive thresholding technique that determines the optimal threshold by analyzing the grayscale histogram of the entire image [31]. It maximizes the between-class variance of foreground and background, requiring no prior threshold setting. It performs well even under low contrast and nonuniform background conditions, effectively separating foreground and background regions, as shown in Figure 5.

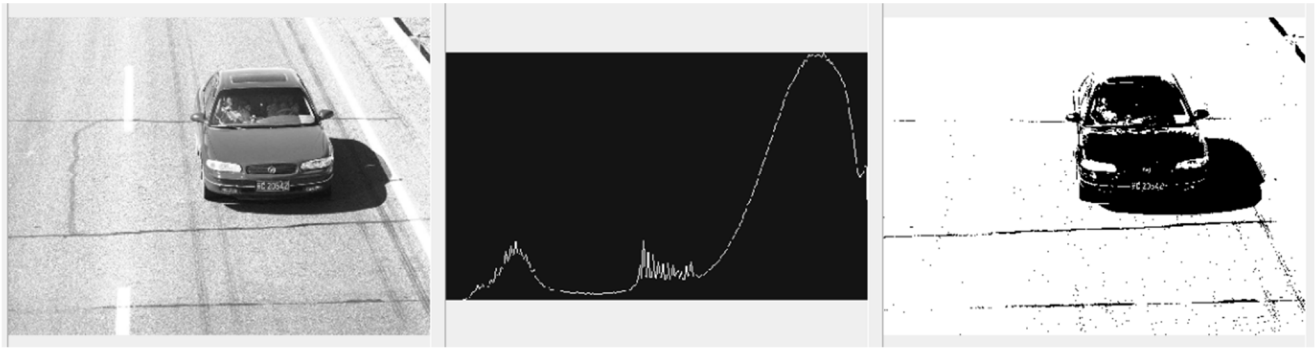


Figure 5. Image processed using the Otsu algorithm.

The Triangle method is another automatic thresholding approach, and is particularly suitable for images with clearly distinguishable object and background regions. It constructs a triangle using the histogram peak and the lowest gray level, then identifies the point farthest from the baseline as the triangle apex. The gray level corresponding to this apex is selected as the threshold. This method is simple and efficient, and works well for unimodal or bimodal histograms, as shown in Figure 6.

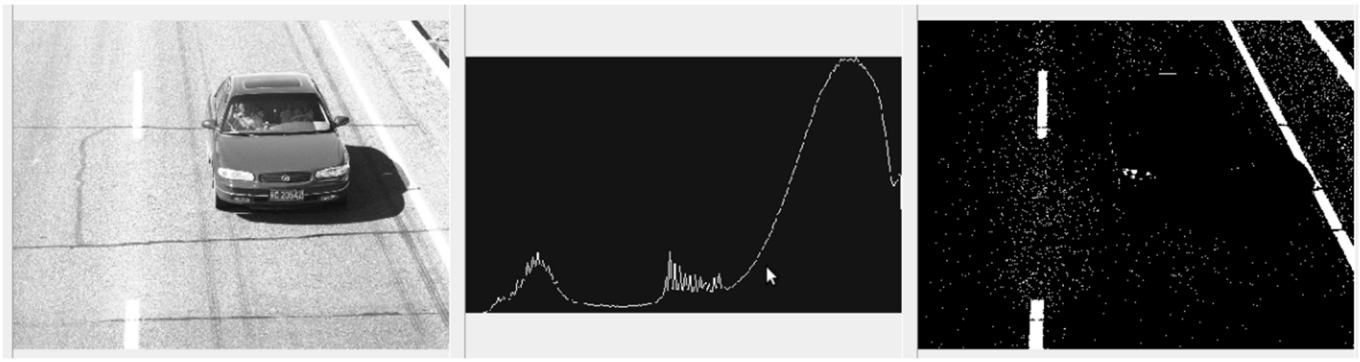


Figure 6. Image processed using the Triangle algorithm.

Both methods are applicable to fluorescence microscopy images to some extent. However, for fluorescence images, intensity distribution is often nonuniform, and relying solely on a single binarization method cannot achieve satisfactory results. A comparison is shown in Figure 7. Therefore, it is necessary to combine binarization algorithms with image enhancement techniques. This integrated approach effectively mitigates non-uniform illumination and further improves the accuracy and efficiency of subsequent image analysis.



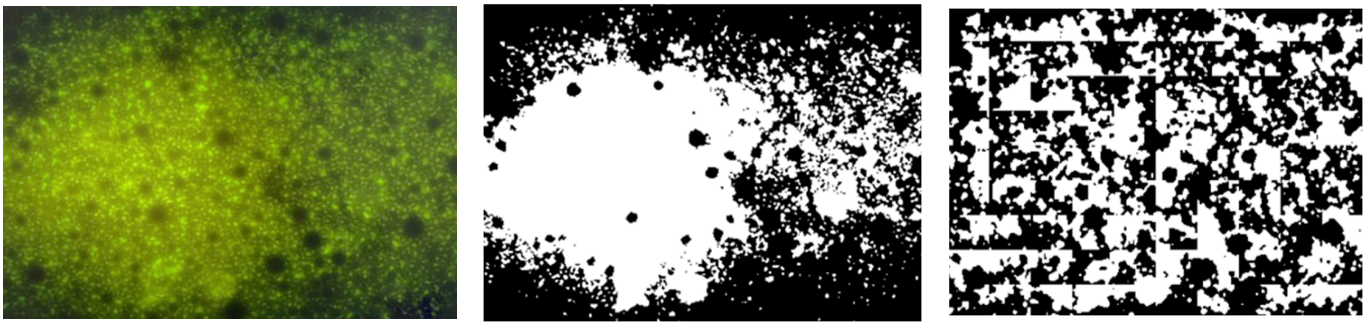
(**a**) Original image (**b**) Triangle algorithm (**c**) Otsu algorithm

Figure 7. Different algorithm processing results.

Segmentation strategy and program optimization: To address the challenge of uneven brightness across different regions, where the fluorescence intensity of the asphalt in brighter areas may be similar to that of modified agents in darker areas, making it difficult for the algorithm to distinguish between them, an image segmentation strategy was adopted in this study. The image was divided into multiple regions to ensure that the features of the modifier within each local area could be effectively highlighted. Through detailed segmentation and subsequent region merging, the spatial distribution of the epoxy resin modifier can be accurately extracted.

The results show that after segmentation, image details are further enhanced and the binarization performance is significantly improved compared with the non-segmented case. However, transitional areas between segments still require further processing. The segmentation strategy provides greater improvement for the Triangle method than for the Otsu method.

Final program design: A comparative analysis of Figures 8 and 9 shows that applying adaptive histogram equalization to the segmented images for smoothing effectively improves image contrast while preserving fine details, thereby providing a better foundation for subsequent binarization. The Triangle thresholding method was then used for the final binarization step. This combined strategy not only improves processing accuracy but also enhances the overall image quality.



(**a**) Original image (**b**) Without segmentation (**c**) After segmentation

Figure 8. Comparison of pre-processing and post-processing results of the Otsu algorithm with image block segmentation.



(**a**) Original image (**b**) Without segmentation (**c**) After segmentation

Figure 9. Comparison of pre-processing and post-processing results of the Triangle algorithm with image block segmentation.

As shown in Figure 10, this integrated algorithm effectively extracts the distribution of epoxy resin within the asphalt while simplifying the image representation. The advantage of this tailored algorithm over conventional methods lies in its ability to effectively distinguish epoxy domains within the dark asphalt matrix under complex illumination conditions (as evidenced by the comparisons in Figures 7–9). More importantly, this study extracts two novel quantitative indicators for the first time: the standard deviation of area, which characterizes the degree of local agglomeration of WER particles, and the distribution uniformity standard deviation, which reflects the global dispersion homogeneity of WER within the matrix. These indicators provide a quantitative bridge between the microstructural state and the macroscopic performance, allowing for a more precise and objective evaluation of the WER modification effect.

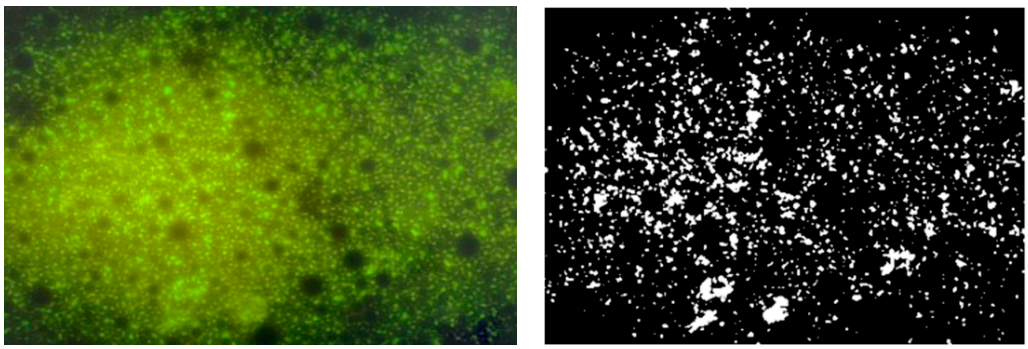


Figure 10. Final processing results.

3. Results and Discussion

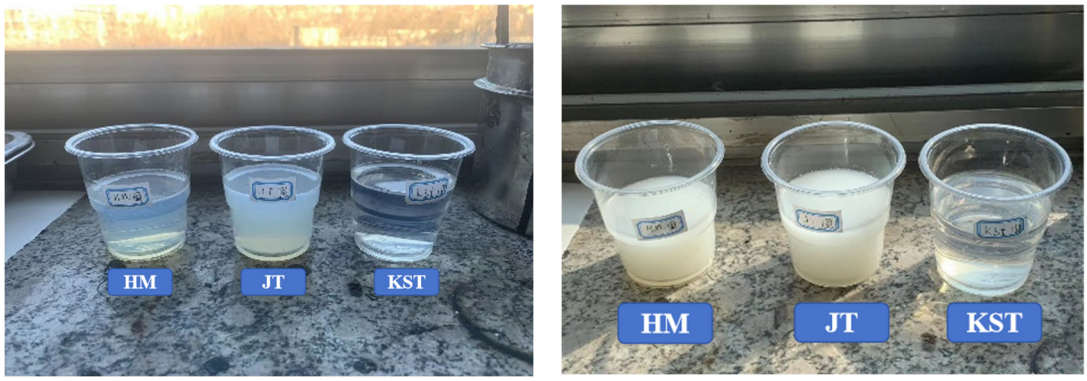
3.1. Performance Evaluation of WERAE

3.1.1. Compatibility Analysis

Considering that WERAE is used on-site, both the WER and the curing agent must meet certain compatibility requirements. Therefore, the compatibility analysis consists of two parts: first, the compatibility between the curing agent and water, which determines whether the curing agent can be uniformly dispersed within a short period; and second, the compatibility between WER and emulsified asphalt, which governs the stability of the blended system.

Water Solubility of Curing Agent

The results show that all three curing agents can be highly dispersed in water to form emulsions rather than true solutions. The dispersion rate follows the order HM ≈ JT > KST, indicating that the curing agents in the HM and JT systems can more readily achieve uniform dispersion within a shorter time frame, whereas the KST curing agent exhibits a relatively slower dispersion rate, likely due to its higher viscosity. As shown in Figure 11, after standing for one day, the HM and JT systems formed visually uniform and stable milky emulsions, whereas the KST system exhibited a slightly non-uniform dispersion with some flocculent aggregates. Nevertheless, no significant macroscopic phase separation occurred in any of the three systems, demonstrating that all three curing agents can form stable dispersions (emulsions) with water.



(**a**) 10 min (**b**) 1 d

Figure 11. Curing agent water solubility test.

The results show that all three curing agents are fully miscible with water in any proportion, indicating excellent water solubility. The dissolution rate follows the order HM ≈ JT > KST, suggesting that the curing agents in the HM and JT systems can more readily achieve uniform dispersion in water within a shorter time frame, whereas the KST curing agent exhibits a relatively slower dissolution rate, likely due to its higher viscosity. After standing for one day, no phase separation was observed in any of the three systems, indicating that all curing agents can form stable mixtures with water.

Compatibility of WER and Emulsified Asphalt

The compatibility between waterborne epoxy resin and emulsified asphalt is commonly evaluated by measuring the particle size distribution of their mixtures.

(1) Particle Size Distribution of the Three Waterborne Epoxy Resins

The laser particle size analysis results of the three waterborne epoxy systems are shown in Figure 12. It can be observed that the particle size distribution curves of all three

systems are located to the left of the emulsified asphalt curve, indicating that the particle sizes of WER are all smaller than those of the emulsified asphalt. The average particle size follows the order KST > HM > JT. Among them, the JT system exhibits the best uniformity, with a balanced proportion of large, medium, and small particles and a distribution close to a normal distribution. The KST system shows a higher proportion of large particles and the poorest uniformity, while the HM system lies between the two. In general, smaller particle size facilitates more uniform dispersion of epoxy resin, thereby influencing its compatibility with emulsified asphalt.

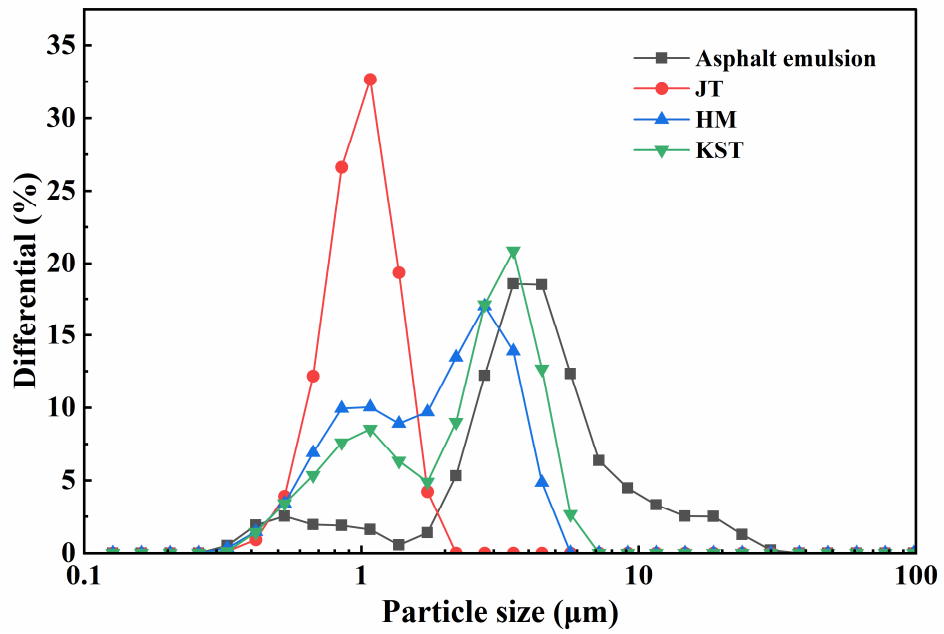


Figure 12. Comparison of particle sizes of three resins and the asphalt emulsion.

(2) Particle Size Distribution of WER and Emulsified Asphalt Mixtures

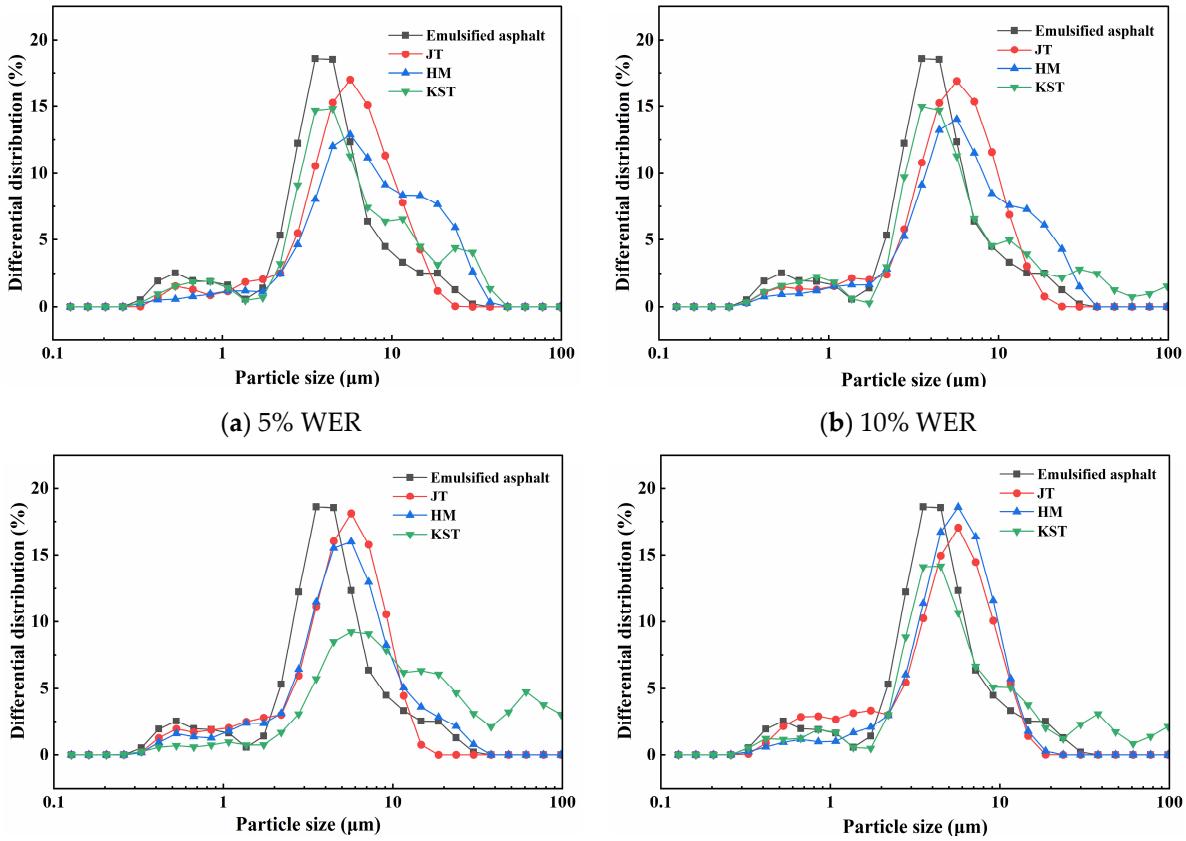
The three waterborne epoxy resins (JT, HM, and KST) were added to the emulsified asphalt at dosages of 5%, 10%, 15%, and 20%, respectively. The particle size distribution results of the modified emulsified asphalt are shown in Figure 13.

It should be noted that since the WER particles are much smaller than the emulsified asphalt droplets, the laser diffraction results represent the combined particle size distribution of both WER particles and asphalt droplets in the mixed system. Although this method does not separate the absolute sizes of the two phases individually, it is highly sensitive in reflecting the formation of coarse particles or aggregates caused by incompatibility between the WER and asphalt. The significant rightward shift of the D90 value in the KST mixture clearly reveals such aggregation behavior.

To ensure the validity of this relative comparison, all samples were prepared using exactly the same low-shear mixing and standardized ultrasonication procedures prior to the laser diffraction measurements. Therefore, any relative differences in the particle size curves between formulations are inherently reliable and effectively reflect the changes in dispersion state induced by the compatibility of the different WER systems, rather than artifacts from sample preparation.

Based on the laser particle size distribution of the mixtures of WER and emulsified asphalt (Figure 13), as well as the average particle size distribution (Figure 14, where D25 represents the particle size at the 25% cumulative distribution, and similarly for other percentiles), it can be observed that after blending JT and HM with the emulsified asphalt, the proportion of fine particles increases, while the overall particle size distribution curve

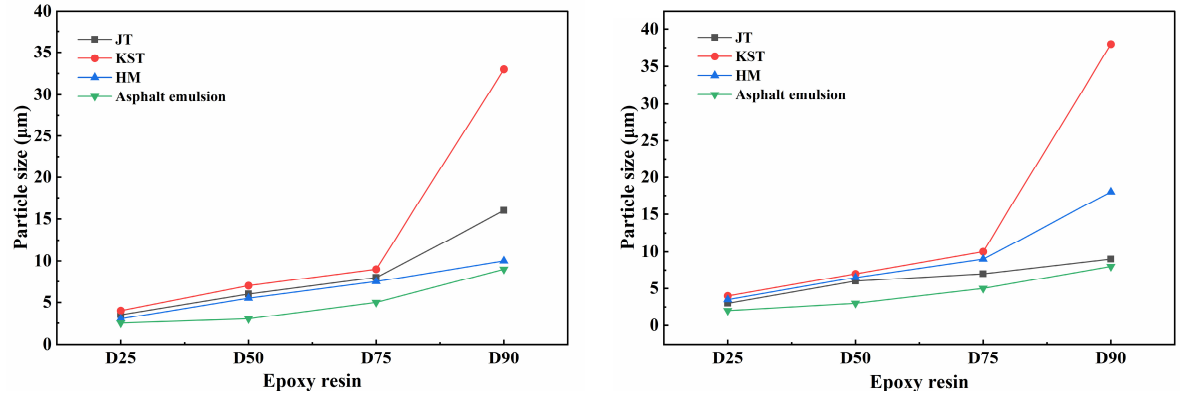
shows little variation and the cumulative distribution curve remains relatively smooth. This suggests that both systems exhibit good compatibility with the emulsified asphalt. The fine particles can fill the voids formed by larger particles, which is beneficial for improving the uniformity and stability of the WERAE system.



(**a**) 5% WER (**b**) 10% WER

(**c**) 15% WER (**d**) 20% WER

Figure 13. Particle size distribution under different WER dosages.



(**a**) 10% WER (**b**) 20% WER

Figure 14. Accumulated particle size distribution.

In contrast, after blending KST with the emulsified asphalt, the proportion of coarse particles increases significantly, and the particle size distribution curve shifts noticeably to the right. The D90 value is substantially higher than that of the other two epoxy systems, indicating that the epoxy resin and emulsified asphalt particles tend to coalesce into larger aggregates rather than being uniformly dispersed between asphalt droplets. This behavior

is unfavorable for the stability of the WERAE system. Emulsified asphalt modified with this epoxy system may undergo premature breaking, leading to early agglomeration and flocculation, which is detrimental to construction workability. This phenomenon may be attributed to the higher electronegativity and the inherently larger particle size of the KST system, which promotes aggregation within the system.

3.1.2. Coating Performance and Strength of WERAE

Film-Forming Performance Evaluation

Due to the poor compatibility of the KST system with emulsified asphalt in the asphalt compatibility tests, it was excluded from subsequent investigations even though it showed a relatively good curing rate and bonding strength in later performance tests. Therefore, further studies were conducted only on the JT and HM systems.

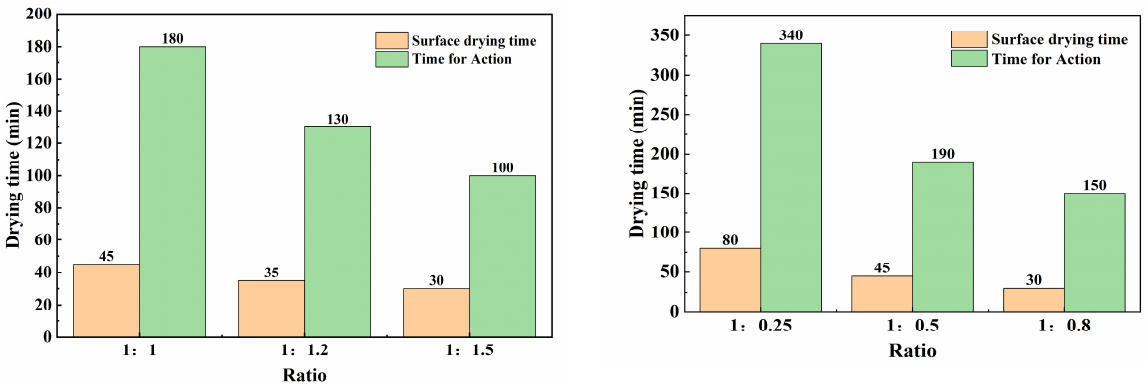
In the curing and crosslinking process, the ratio between waterborne epoxy resin and curing agent plays a crucial role in determining the quality of the final cured product. An insufficient amount of curing agent leads to incomplete reactions, while an excessive amount may cause excessively rapid local reactions, resulting in non-uniform products. Therefore, an appropriate mixing ratio is essential.

Theoretically, an optimal stoichiometric relationship exists, expressed as:

$$\text{Resin mass} = (\text{Curing agent mass} \times \text{Epoxy equivalent})/\text{Active hydrogen equivalent}$$

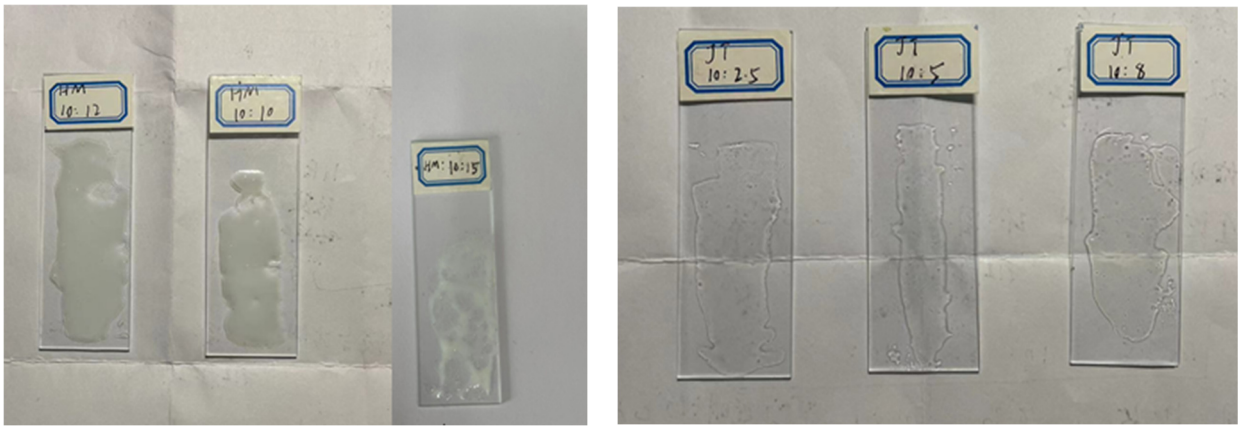
At this condition, the amine groups and epoxy groups react completely. The epoxy equivalent and active hydrogen equivalent are key parameters for characterizing waterborne epoxy systems and can be used to calculate the theoretical mixing ratio. However, in practice, both values are given as ranges, and the theoretical ratio is also expressed as an interval. The final optimal ratio must therefore be determined experimentally. Based on the theoretical calculation, the mixing ratio ranges of the two waterborne epoxy systems were obtained, and three levels (high, medium, and low) were selected for experimental verification.

The measured surface drying time and hard drying time of the two waterborne epoxy systems are shown in Figure 15. The results indicate that the HM system exhibits a slightly faster reaction rate than the JT system. Figure 16 presents the curing and film-forming states of the two systems, showing that the HM system performs less uniformly in coating formation compared with the JT system.



(**a**) HM system (**b**) JT system

Figure 15. Surface drying time and actual drying time of the two waterborne epoxy systems.



(**a**) Film morphology of HM system (**b**) Film morphology of JT system

Figure 16. Two film-forming states of the waterborne epoxy systems.

In addition, Tables 6 and 7 evaluate the coating performance of the two waterborne epoxy systems in terms of hardness and volume change of the cured products. Under the same testing time, a harder cured product generally indicates a faster reaction rate; therefore, the JT system demonstrates a higher curing speed. During the curing process, the volume of the cured product typically undergoes shrinkage, which is mainly attributed to the gradual evaporation of water in the system. However, excessive volume shrinkage is unfavorable for strength development in WERAE. In this study, the degree of volume shrinkage is classified, from low to high, as no shrinkage, slight shrinkage, minor shrinkage, moderate shrinkage, and significant shrinkage. The results show that the HM system exhibits more pronounced volume changes, whereas the JT system only shows significant shrinkage when the curing agent content reaches the upper theoretical limit. This indicates that the JT system exhibits more stable curing behavior.

Table 6. Coating performance of the HM system.

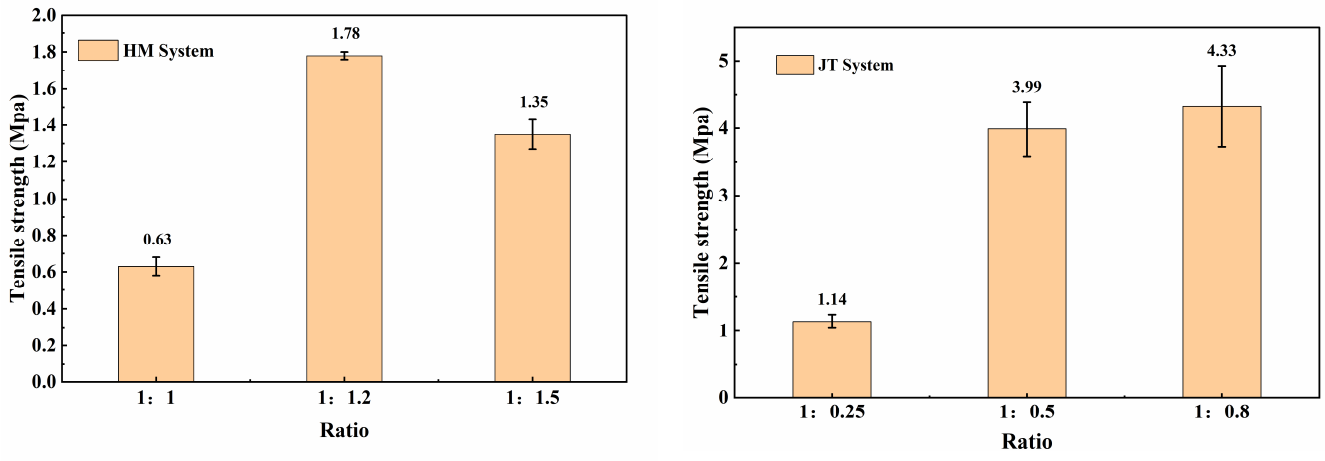
Ratio (Resin:Hardener)	1:1	1:1.2	1:1.5
Hardness of cured product (12 h)	Soft	Relatively soft	Hard
Volume shrinkage (1 d)	Significant shrinkage	Significant shrinkage	Moderate shrinkage
Volume shrinkage (3 d)	Significant shrinkage	Moderate shrinkage	Moderate shrinkage

Table 7. Coating performance of the JT system.

Ratio (Resin:Hardener)	1:0.25	1:0.5	1:0.8
Hardness of cured product (12 h)	Relatively soft	Hard	Very hard
Volume shrinkage (1 d)	No shrinkage	Slight shrinkage	Minor shrinkage
Volume shrinkage (3 d)	No shrinkage	Slight shrinkage	Significant shrinkage

Bonding Strength

Bonding strength is a direct indicator of the mechanical strength of the cured product. A pull-off strength test was conducted using a Posi Test AT-A adhesion tester, and the results are shown in Figure 17.



(**a**) Pull-off strength of the M system (**b**) Pull-off strength of the JT system

Figure 17. Pull-off strength of the two waterborne epoxy systems.

The pull-off test results show that, regardless of whether the ratio of epoxy resin to curing agent is high, medium, or low, the JT waterborne epoxy system consistently exhibits higher bonding strength than the HM system. When the curing agent content is relatively low, the bonding strengths of the two systems are comparable. As the curing agent content further increases, the HM system reaches a peak in bonding strength, whereas the JT system shows a significant improvement, demonstrating better application potential.

To identify the optimal resin-to-curing-agent ratio for the JT system, the mixing proportions were further refined. The final bonding strength of the cured products is shown in Figure 18. As the curing agent content increases, the bonding strength first increases and then decreases. This trend may be attributed to excessive curing agent leading to excessively rapid local reactions, which hinder the continuation and uniformity of the curing process. The optimal bonding performance is achieved when the epoxy-resin-to-curing-agent ratio is 1:0.6.

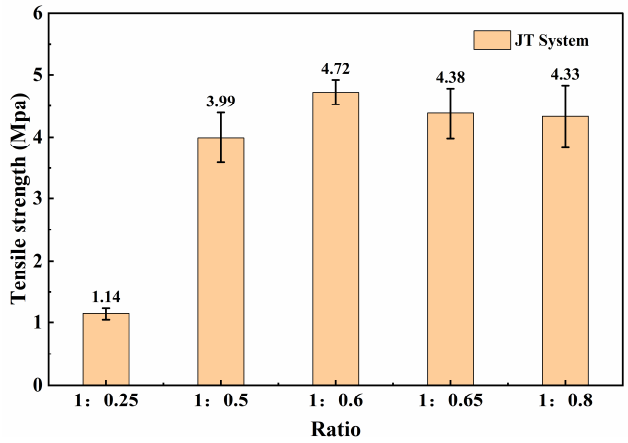


Figure 18. The tensile strength of the JT system with different ratios.

3.2. Rheological Behavior Analysis

Although only one test was performed for each formulation, each test was conducted strictly following the standard protocol. Pre-experimental strain sweeps were conducted for every sample to ensure that the measurements were performed in the linear viscoelastic region, which guarantees the validity of the rheological trends observed. Asphalt is a viscoelastic material. At low temperatures, it exhibits high stiffness and elasticity, behaving more like a solid and showing strong resistance to deformation. At high temperatures,

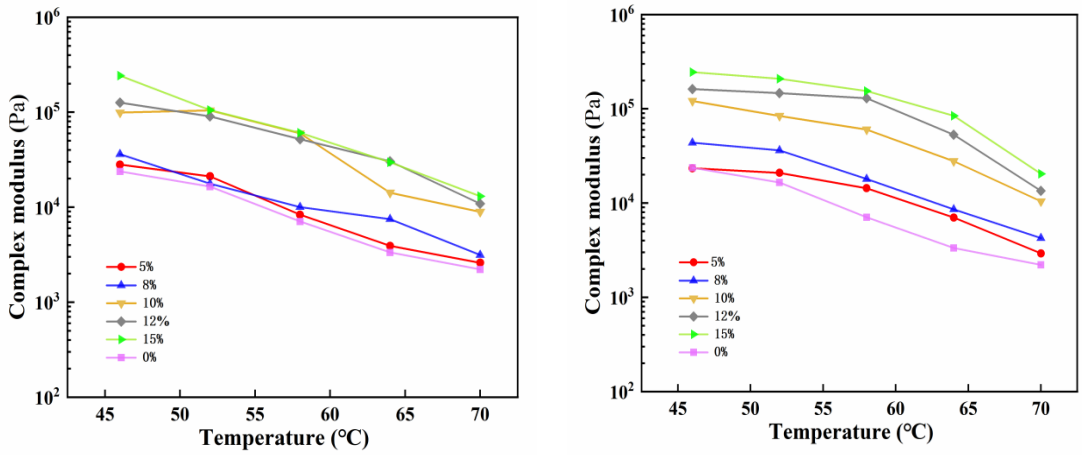
asphalt displays more viscous characteristics, behaving more like a fluid that can flow and deform under external loads. An ideal asphalt material should maintain appropriate viscoelasticity over a wide temperature range. For WERAE, the incorporation of epoxy resin introduces thermosetting characteristics, making conventional performance indices less effective in reflecting its true behavior. The dynamic modulus principal curve is of great significance for repair design and for predicting fatigue and permanent deformation strains [32]. It has become an important method in current research.

Among the rheological parameters, the complex modulus G^* is a comprehensive indicator of viscoelastic behavior, representing the overall resistance of a material to shear deformation. A higher complex modulus indicates stronger deformation resistance. The phase angle δ is the phase difference between stress and strain waveforms, reflecting whether the material behavior is more elastic or viscous; a smaller phase angle indicates more elastic behavior, while a larger phase angle indicates more pronounced viscous behavior.

3.2.1. Analysis of Temperature Sweep Results

(1) Complex Modulus

From Figure 19, it can be observed that for all WERAE formulations, the complex shear modulus decreases with increasing test temperature. This behavior is attributed to the strong temperature sensitivity of the asphalt, which exhibits clear thermo-rheological dependence. At low temperatures, the asphalt shows higher elasticity because molecular motion is restricted and intermolecular interactions are stronger. As temperature increases, molecular mobility is enhanced and intermolecular interactions weaken, leading to increased fluidity.



(**a**) WERAE (**b**) WERAE + 3% SBR

Figure 19. Complex modulus varies with temperature.

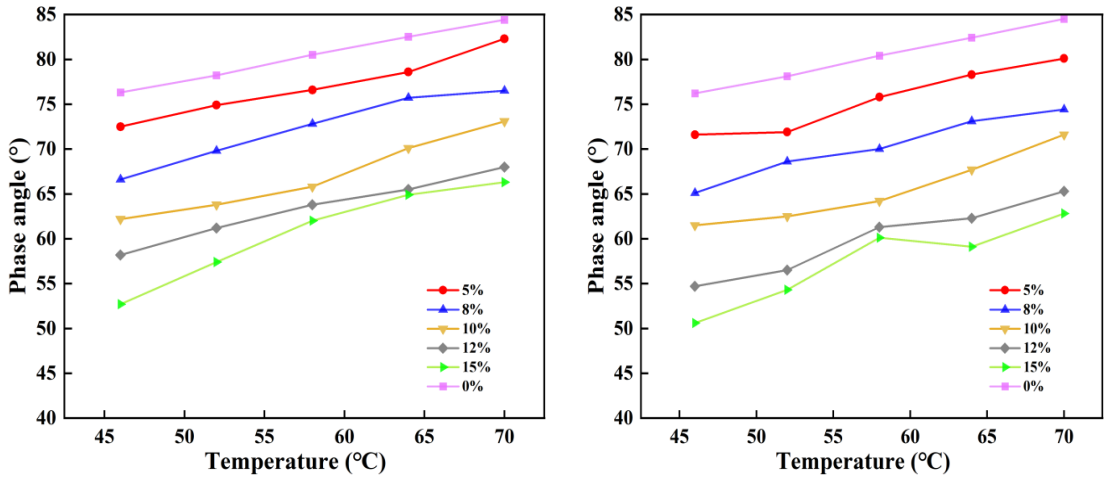
At the same temperature, a higher WER content results in a larger complex shear modulus. This is because epoxy resin is a thermosetting material; once incorporated into the asphalt, through the curing reaction, the epoxy resin cures into a three-dimensional spatial network morphology within the asphalt matrix. This cured structure significantly increases material stiffness. The formation of this network shows a clear increasing trend in terms of material stiffness and the complex modulus. The crosslinked structure restricts molecular chain mobility, thereby increasing the elastic response under loading.

The addition of WER reduces the high-temperature flowability of the asphalt mixture, enabling it to maintain a higher modulus over a wider temperature range and thus retain better performance even under elevated temperatures. When the WER content is relatively low (<8%), the improvement in the complex modulus is not significant, as a continuous

crosslinked network has not yet formed. The incorporation of SBR further increases the complex modulus at the same epoxy content. This may be attributed to the physical entanglement or interaction between the three-dimensional epoxy network formed after curing and SBR molecules, resulting in a more stable and denser network structure.

(2) Phase Angle

As shown in Figure 20, with increasing epoxy resin content, the phase angle exhibits a decreasing trend regardless of whether SBR is incorporated. This indicates that a higher epoxy resin content is more favorable for improving the material's resistance to permanent deformation.



(**a**) WERAE (**b**) WERAE + 3% SBR

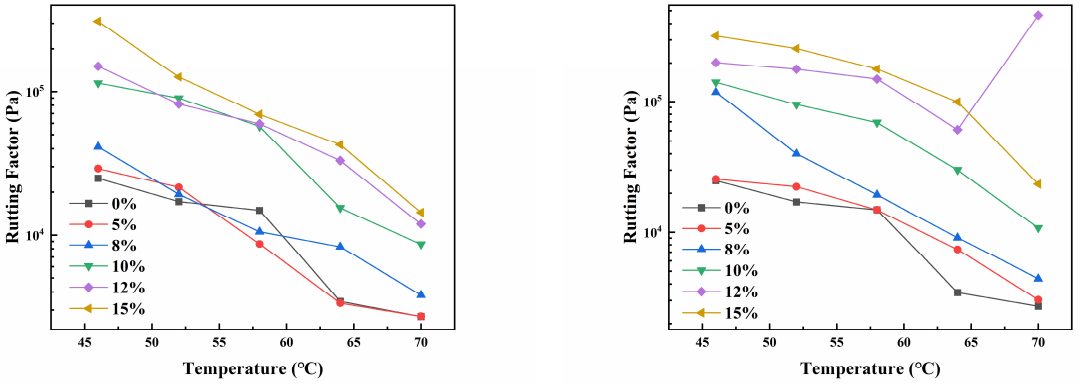
Figure 20. Variation in phase angle with temperature.

From the temperature-dependent variation in the phase angle, it can be observed that an increase in temperature enhances the viscous component, making the material's response to shear stress more flow-like, and thus leading to an increase in phase angle. The magnitude of this increase is generally around 10°. In addition, the phase angle of SBR-WERAE is slightly lower than that of the samples containing only WER.

In terms of the variation in amplitude, SBR-WERAE generally shows a slightly smaller increase compared with WERAE. Notably, at a WER content of 15%, the increase in phase angle for SBR-WERAE is significantly lower than that of WERAE, indicating that the incorporation of SBR can reduce the temperature sensitivity of the asphalt material and help maintain its elastic performance.

(3) Rutting Factor (G*/sinδ)

As shown in Figure 21, the rutting factor (G*/sinδ) follows a decreasing trend similar to that of the complex modulus as temperature increases. Under the same test temperature, increasing the WER content leads to a significant enhancement in the rutting factor, indicating a substantially improved resistance to high-temperature permanent deformation. Notably, at 58 °C, the rutting factor of the 10% WER + 3% SBR mixture is significantly higher than that of the base asphalt, and the enhancement is also remarkably greater than that observed with WER alone. This confirms that the addition of SBR synergistically reinforces the epoxy network structure, further improving the high-temperature stability of the modified binder.

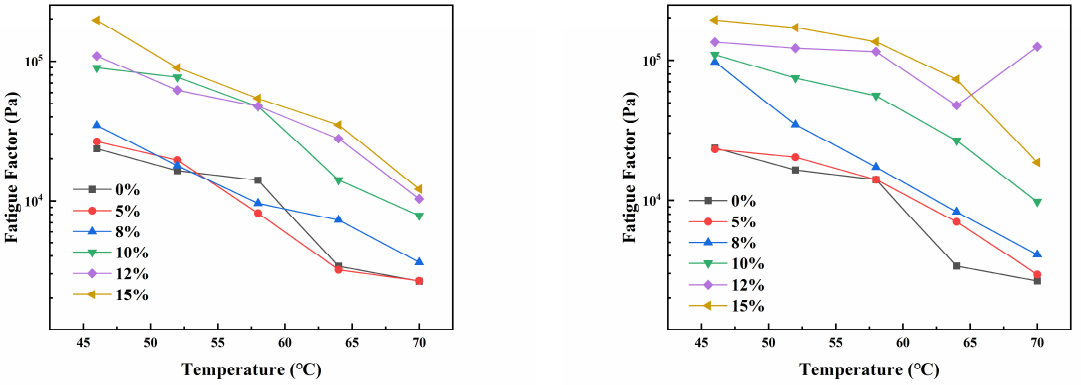


(**a**) WERAE (**b**) WERAE + 3% SBR

Figure 21. Variation in rutting factor with temperature.

(4) Fatigue Factor (G*·sinδ)

As presented in Figure 22, the fatigue factor (G*·sinδ) also increases with higher WER content, primarily driven by the significant rise in G* due to the formation of the cured epoxy microstructure. According to the Superpave specifications, a higher fatigue factor typically indicates increased stiffness, which may theoretically reduce the resistance to fatigue cracking under repeated loading. However, it is important to note that the magnitude of the increase in the rutting factor is substantially larger than that of the fatigue factor across all temperature ranges. This suggests that the enhancement in high-temperature anti-rutting performance is far more pronounced than any potential negative impact on fatigue resistance within the tested WER content range. The microscopic network of WER effectively improves the overall high-temperature resistance of the asphalt binder without causing a significant degradation in its susceptibility to fatigue damage.



(**a**) WERAE (**b**) WERAE + 3% SBR

Figure 22. Variation in fatigue factor with temperature.

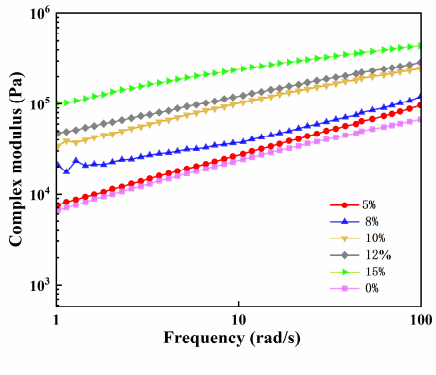
3.2.2. Analysis of Frequency Sweep Results

Frequency sweep tests are conducted by varying the loading frequency applied to asphalt materials while keeping the temperature constant. This test reveals the material response under different loading rates and is particularly useful for evaluating the influence of traffic loading speed on asphalt performance.

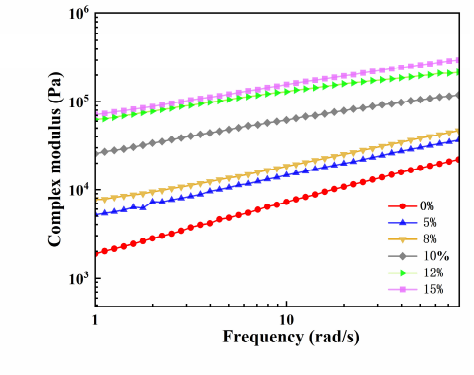
(1) Complex Modulus

Figure 23 presents the variation in the complex modulus of modified asphalt samples with different epoxy resin contents under frequency sweep tests at various temperatures.

It can be observed that as the frequency increases from 1 rad/s to 100 rad/s, the complex modulus of all samples increases accordingly. The frequency dependence of the modulus follows a well-defined power-law relationship, which is consistent with the viscoelastic behavior of asphalt, indicating that asphalt tends to exhibit more elastic response at higher strain rates. This reflects an enhanced resistance to deformation under higher shear loading rates.

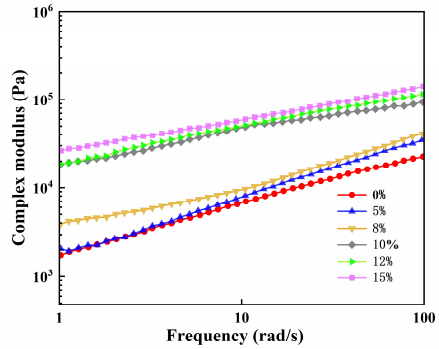


(**a**$_1$) WERAE

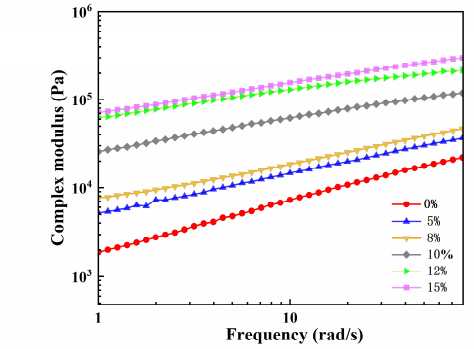


(**a**$_2$) WERAE + 3% SBR

(**a**) 46 °C

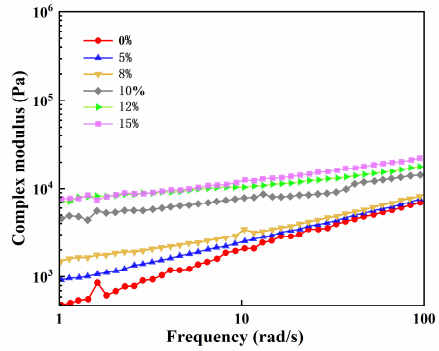


(**b**$_1$) WERAE

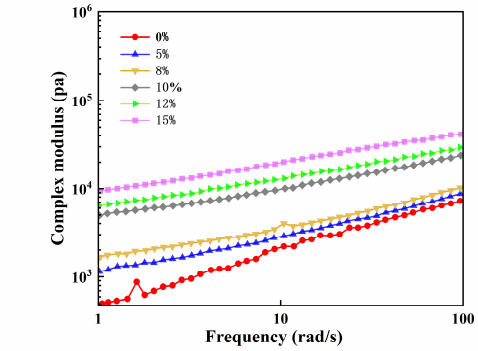


(**b**$_2$) WERAE + 3% SBR

(**b**) 58 °C



(**c**$_1$) WERAE



(**c**$_2$) WERAE + 3% SBR

(**c**) 70 °C

Figure 23. Frequency-dependent variation in the complex modulus of WERAE with different mix proportions. (Note: To ensure visual clarity of the multi-line overlays, standard deviation (SD) error bars are not explicitly plotted on this figure. All statistical significance ($p < 0.05$) and SD values used for ANOVA tests are derived from three replicates.).

The epoxy resin content has a significant effect on increasing the complex modulus. The modified asphalt with 15% epoxy resin content exhibits the highest complex modulus across the entire frequency range. After the addition of SBR, the complex modulus of the modified emulsified asphalt is further improved, with a more pronounced effect at lower epoxy resin contents. The base asphalt (0% content) is the most sensitive to frequency changes, while increasing epoxy resin content gradually reduces this sensitivity, as reflected by the decreasing slope of the curves. At higher modifier contents, the asphalt exhibits weaker frequency dependence, suggesting a more stable internal structure under rapid loading conditions. This is likely attributed to the crosslinked network formed by the epoxy resin.

Overall, the incorporation of epoxy resin significantly improves the mechanical performance of asphalt materials under medium- to high-frequency loading conditions. This enhancement is particularly beneficial for pavement structures subjected to high-temperature environments and high-speed traffic, as it helps reduce rutting and other deformation-related distresses commonly associated with rapid loading and elevated temperatures.

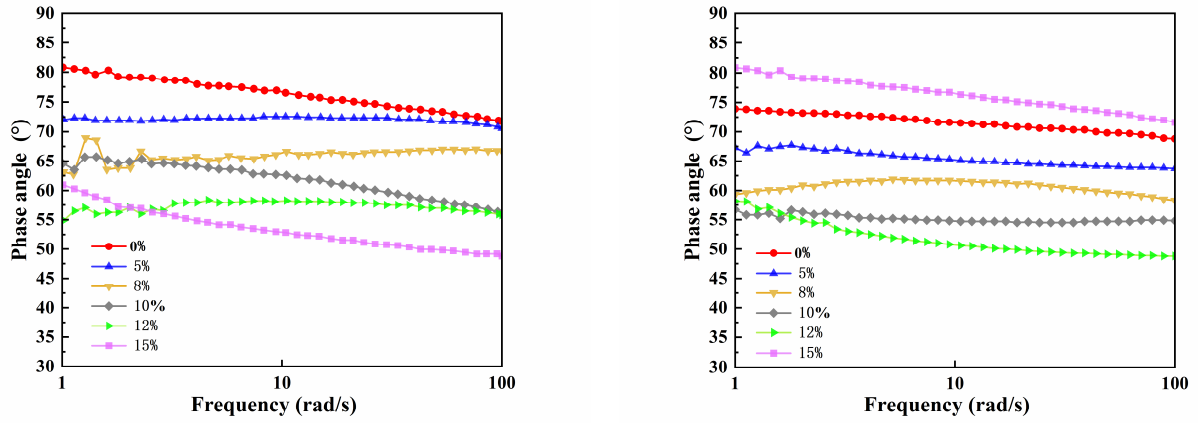
(2) Phase Angle

Figure 24 shows the variation in phase angle with frequency for modified asphalt with different epoxy resin contents under frequency sweep tests. At a relatively low temperature (46 °C), the phase angle of all samples decreases with increasing frequency, which is consistent with the typical viscoelastic behavior of asphalt. This indicates that under higher loading frequencies, the material tends to exhibit a more elastic response.

It is noteworthy that increasing epoxy resin content leads to a significant reduction in phase angle across the entire frequency range, with a more pronounced effect at higher frequencies. This reflects that epoxy resin shows a clear increasing trend in the elastic response of the material while reducing its viscous behavior. The most significant reduction is observed at 15% epoxy resin content, indicating that this proportion maximizes the enhancement of elastic characteristics. In contrast, the base asphalt (0% content) exhibits the highest phase angle, indicating a stronger viscous response under rapid deformation.

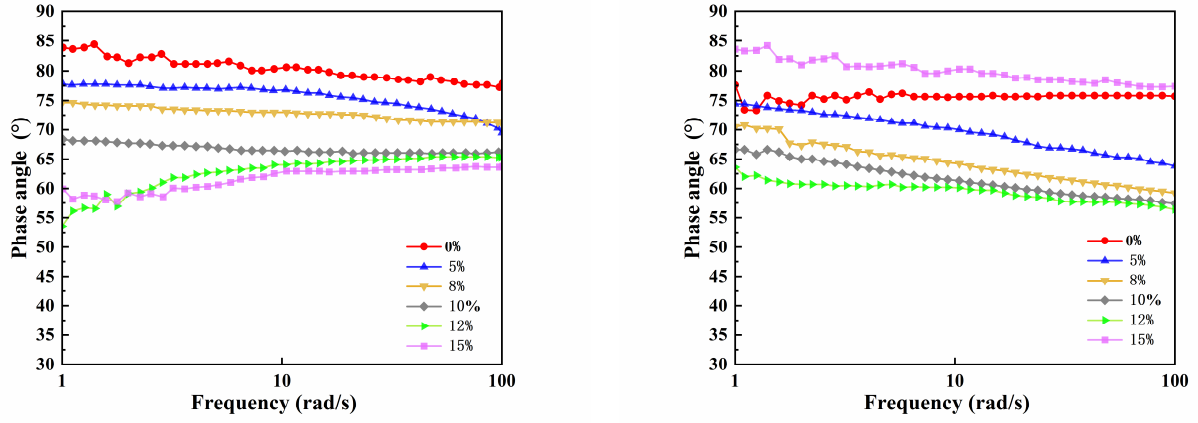
With increasing temperature, some samples show an opposite trend, where the phase angle increases with frequency, such as the 12% and 15% WER samples at 58 °C. In contrast, WERAE modified with SBR maintains a relatively stable elastic response. SBR is a synthetic rubber, and its incorporation increases the elasticity of asphalt mixtures. This may be attributed to the ability of SBR molecular chains to absorb and dissipate energy, thereby reducing permanent deformation caused by dynamic loading. The addition of SBR improves the performance of asphalt mixtures over a wide temperature range, particularly at high temperatures, where it helps maintain elasticity and resist deformation under repeated traffic loading.

At 70 °C, all modified asphalt samples exhibit an increasing phase angle with increasing frequency. This behavior differs from the typical response of viscoelastic materials, which usually show decreasing phase angles with increasing frequency, indicating a more elastic-dominated response. The observed increase suggests that viscous behavior becomes more dominant under these high temperature and frequency conditions. This may be due to partial loosening of the epoxy crosslinked network at 70 °C, leading to increased flow behavior under stress. Although all samples follow a similar trend, the phase angle decreases with increasing epoxy resin content, indicating that epoxy resin still enhances the elastic modulus even at elevated temperatures. The addition of SBR further delays the relaxation of the epoxy network, contributing to improved high-temperature stability.



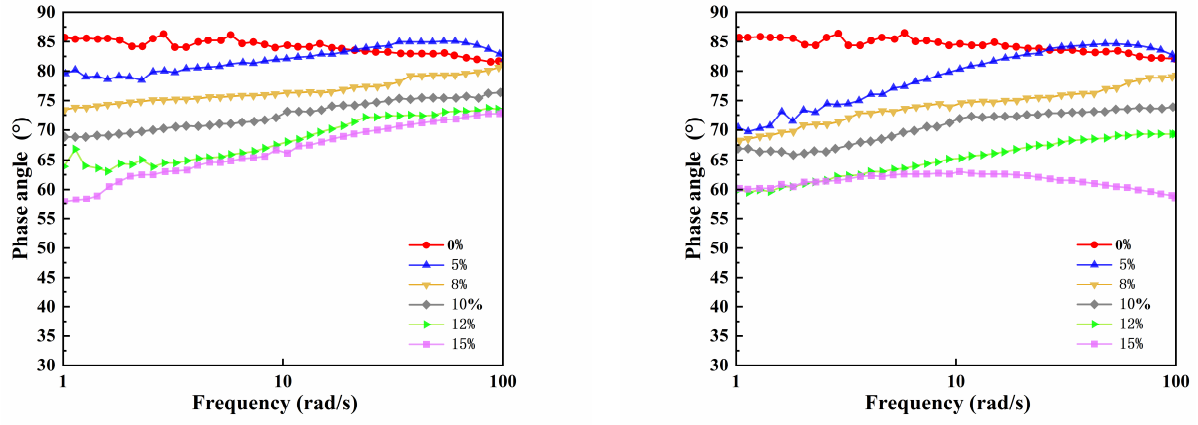
(**a**$_1$) WERAE (**a**$_2$) WERAE + 3% SBR

(**a**) 46 °C



(**b**$_1$) WERAE (**b**$_2$) WERAE + 3% SBR

(**b**) 58 °C



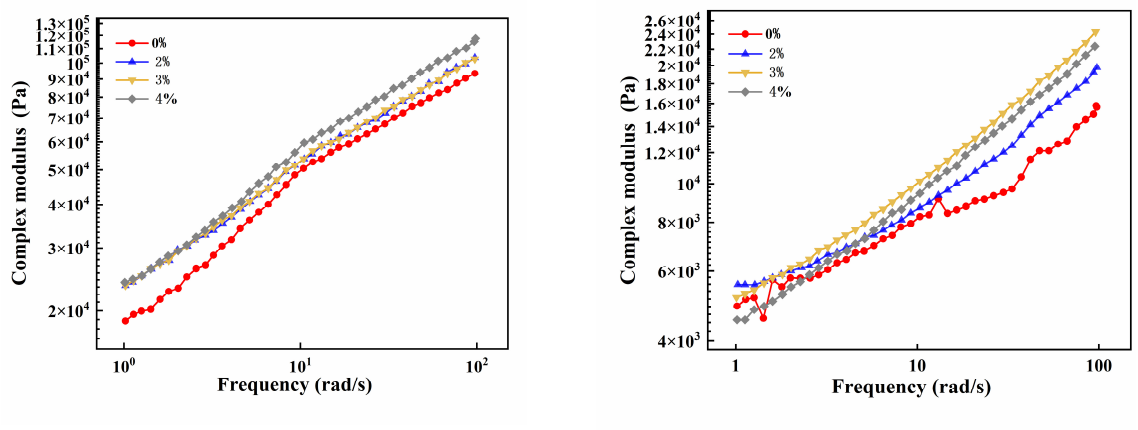
(**c**$_1$) WERAE (**c**$_2$) WERAE + 3% SBR

(**c**) 70 °C

Figure 24. Frequency-dependent variation in phase angle of WERAE with different mix proportions.

3.2.3. Frequency Sweep with Different SBR Contents

To investigate the effect of SBR content on the performance of WERAE, frequency sweep tests were conducted on samples with 10% WER and varying SBR contents of 2%, 3%, and 4%. The results are shown in Figure 25. From the variation curves of the complex modulus, all mixtures exhibit a similar overall trend. With increasing SBR content, the complex modulus first increases and then decreases. The mixture with 3% SBR shows the optimal viscoelastic performance. This behavior may be related to the molecular structure of SBR and the network it forms within the asphalt matrix. At 3% content, the asphalt mixture demonstrates excellent performance under both high- and low-frequency conditions, indicating a balanced combination of elasticity and deformation resistance under dynamic loading. However, when the SBR content is too high, the complex modulus decreases, which may be attributed to excessive SBR increasing the viscous component of the system and thereby reducing efficient load transfer within the material. While the enhanced adhesion does not directly equate to long-term water stability, it provides a strong indication that WERAE, especially with SBR, may exhibit superior resistance to moisture-induced stripping in actual pavement applications.



(**a**) 58 °C (**b**) 70 °C

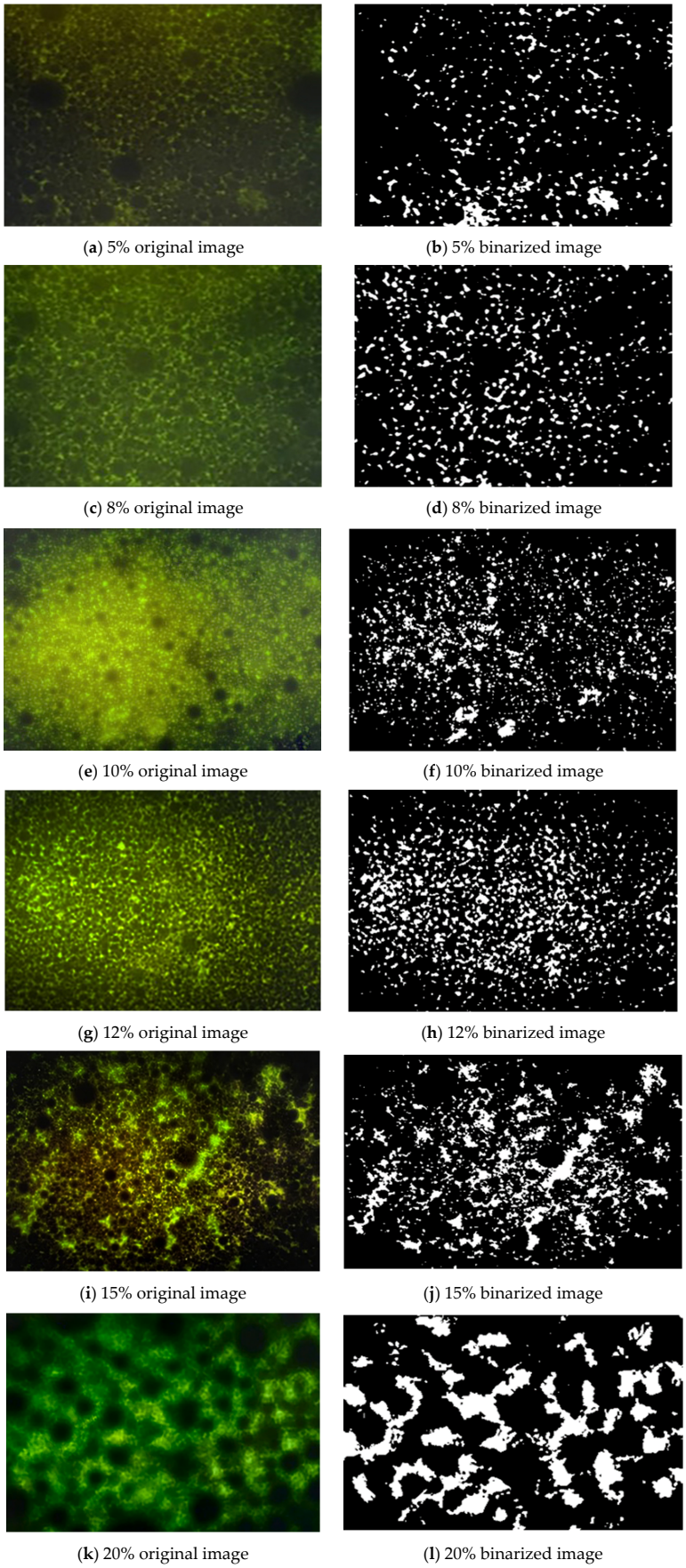
Figure 25. Frequency sweep results with different SBR contents.

3.3. Microstructural and Surface Characterization Analysis

While the fluorescence microscopy in this study primarily reveals the spatial distribution of epoxy domains, the underlying chemical interactions between WER and asphalt have been documented in previous works. For instance, Cong et al. [15] systematically characterized the morphology and glass transition temperature of epoxy-modified asphalt binders, confirming the significant influence of curing temperature on the crosslinking behavior. More importantly, Cuadri et al. [20] revealed through FTIR and SARA analysis that esterification and etherification reactions occur between epoxy resin and the aromatic/resin fractions in asphalt, forming high-molecular-weight compounds. These established chemical mechanisms provide a theoretical basis for the thermosetting characteristics and enhanced interfacial bonding observed in the present WERAE system.

3.3.1. Qualitative Observation

The fluorescence micrographs of samples with different epoxy resin contents and their corresponding binary images are shown in Figure 26. Since SBR does not exhibit fluorescence under the test conditions, the fluorescence characteristics of WERAE and WERAE with 3% SBR are essentially similar at the same epoxy resin content. Therefore, this section focuses on discussing the fluorescence results of WERAE with 3% SBR.



(**a**) 5% original image (**b**) 5% binarized image

(**c**) 8% original image (**d**) 8% binarized image

(**e**) 10% original image (**f**) 10% binarized image

(**g**) 12% original image (**h**) 12% binarized image

(**i**) 15% original image (**j**) 15% binarized image

(**k**) 20% original image (**l**) 20% binarized image

Figure 26. Fluorescence micrographs and corresponding binarized images of WERAE with different mix proportions.

The fluorescence images indicate that as the epoxy resin content increases, the crosslinked network structure of epoxy within the asphalt becomes increasingly pronounced. At low epoxy contents, epoxy particles are mainly dispersed in a dot-like form within the asphalt matrix. When the epoxy resin content reaches 8%, the network structure begins to emerge. At 10% and 12% contents, the network becomes more distinct and continuous. At 15% content, aggregation of epoxy domains can be observed, and this aggregation becomes even more pronounced when the content increases to 20%.

3.3.2. Area Fraction of Epoxy Resin

The area fraction of the epoxy resin modifier is a key indicator for evaluating its modification effectiveness. This parameter directly reflects the proportion of modifier present in the asphalt, helping to identify any potential loss of modifier during the preparation process. It is determined by measuring the area of fluorescent regions, which is implemented in the image-processing procedure by calculating the proportion of white regions in the binarized images.

Figure 27 illustrates the variation in the fluorescent area fraction after binarization with increasing waterborne epoxy resin content. It can be observed that the fluorescent area fraction shows good agreement with the epoxy resin dosage. Meanwhile, the measured fluorescent area fraction is slightly higher than the actual epoxy resin content. This discrepancy may be attributed to the projection of the three-dimensional crosslinked network onto a two-dimensional image, as well as the formation of new structures during the curing reaction between the epoxy resin and curing agent, which also exhibit fluorescence. As a result, the calculated fluorescent area fraction appears elevated. Nevertheless, the statistical analysis of the fluorescent area remains effective in reflecting the distribution characteristics of the epoxy resin within the asphalt matrix.

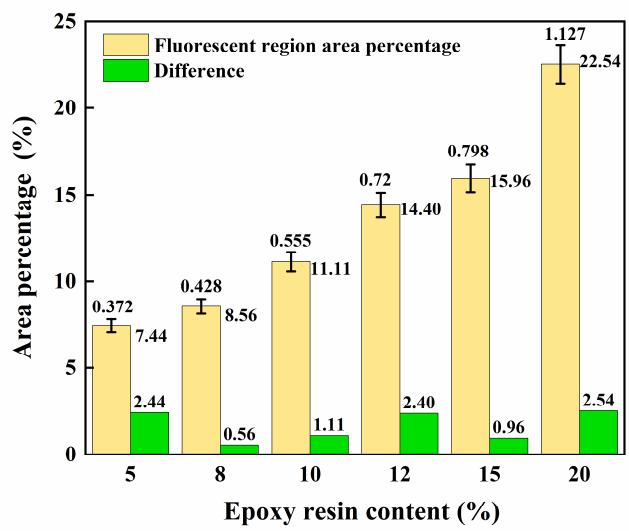


Figure 27. Variation in WER area fraction. (Note: Error bars represent the standard deviation (SD) of the fluorescent region area percentage derived from five random fields of view (n = 5). The green bars denote the positive difference between the measured area percentage and the actual WER content.).

3.3.3. Standard Deviation of Area

The standard deviation of dispersion is used to characterize the degree of local concentration of the modifier within the asphalt, and it is quantified using the standard deviation

of area. A larger value indicates greater variation in the size of epoxy resin aggregation regions, reflecting a higher level of localized clustering. The formula is as follows:

$$\sigma = \sqrt{\sum (P_i - \overline{P})/(N-1)} \quad (1)$$

where P_i is the area of each modifier particle (i.e., the number of pixels in the white regions of the binarized image), $\overline{P}$ is the average particle area, and N is the total number of modifier particles.

Using the "Find Contours" function in the Open CV library, the contours of fluorescent regions can be effectively identified, allowing the area of each fluorescent particle to be calculated. Based on these measurements, the standard deviation of particle area is then computed using the above formula. The results are presented in Figure 28.

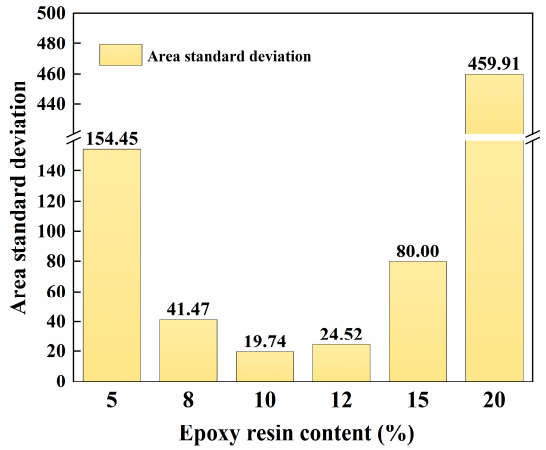


Figure 28. Variation in area standard deviation with WER content.

The analysis results show that the standard deviation of area exhibits a trend of first decreasing and then increasing. At a low epoxy resin content of 5%, the standard deviation is relatively large, which can be attributed to the insufficient amount of epoxy resin to achieve uniform dispersion within the asphalt.

When the epoxy content ranges from 8% to 12%, the variation in standard deviation is relatively small, indicating a more uniform particle size distribution and better dispersion. However, at 15% content, the standard deviation increases significantly, suggesting the onset of local aggregation of larger epoxy particles. At 20% content, the standard deviation rises sharply, showing an order-of-magnitude increase compared to lower contents. This indicates a pronounced difference in particle sizes and a substantial reduction in dispersion uniformity.

According to the ANOVA ($p < 0.05$), the area standard deviation shows no statistically significant difference among the 8%, 10%, and 12% WER groups ($p > 0.05$). However, when the WER content reaches 15%, the area standard deviation exhibits a statistically significant increase compared to the 12% group ($p < 0.05$), confirming that 15% is the critical threshold for severe local agglomeration. These findings are consistent with earlier observations during the preparation of WERAE, where higher epoxy resin contents were found to cause a rapid reduction in flowability within a short period.

3.3.4. Distribution Uniformity

Distribution uniformity is an indicator used to describe the overall dispersion of the modifier within the asphalt matrix. To quantify this characteristic, the observation field of the asphalt sample is divided into multiple square regions of equal size. Within each

subregion, the area fraction of modifier particles is calculated. The standard deviation of these area fractions is then used to evaluate the distribution uniformity of the epoxy resin.

A smaller standard deviation indicates a more uniform distribution of epoxy resin, while a larger value suggests poorer uniformity. In this study, all images are consistently divided into a 4 × 3 grid of equal-sized rectangular regions. The formula for calculating distribution uniformity is as follows:

$$\sigma_0 = \sqrt{\sum (A_i - \overline{A})/(M-1)} \quad (2)$$

where A_i represents the total area of modifier particles within each subregion, $\overline{A}$ is the average value of A_i, and M is the total number of grid cells.

As shown in Figure 29, the standard deviation of distribution uniformity remains at a relatively low level when the epoxy resin content is below 10%. When the epoxy resin content increases to 12%, a noticeable rise in the standard deviation is observed, indicating a reduction in distribution uniformity. As the content further increases from 15% to 20%, the standard deviation increases again significantly, suggesting a further deterioration in the overall dispersion uniformity of the epoxy resin within the asphalt matrix. Combining the macroscopic rheological data and microstructural evaluation, it can be concluded that the 10−12% WER content provides the best trade-off between performance enhancement and structural homogeneity, while 15% acts as a strict upper limit. Similarly, the distribution uniformity standard deviation remains relatively stable, with no significant differences among the groups below 10% WER ($p > 0.05$). However, a statistically significant deterioration ($p < 0.05$) is observed when the content increases to 12%, indicating that the WER content should be controlled below 12% to maintain uniform dispersion. The calculation of this set of parameters helps to comprehensively understand the distribution of the modifier within the asphalt matrix, providing a scientific basis for further optimization of the process of preparing modified asphalt.

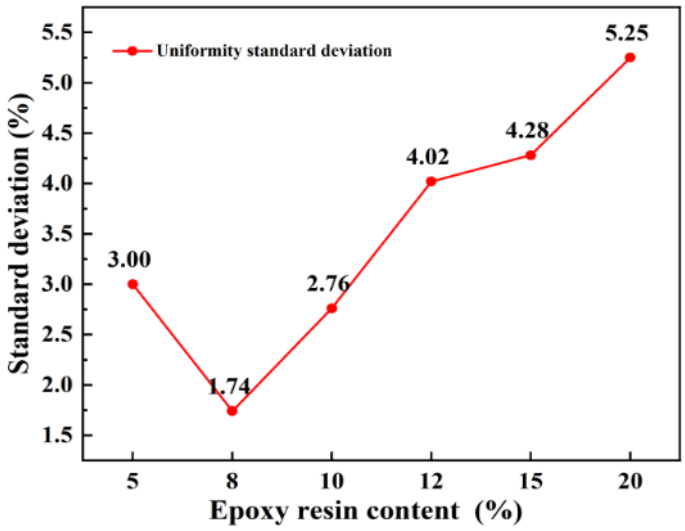


Figure 29. Variation in uniformity standard deviation with WER content.

As shown in Figure 30, the quantitative correlation between macroscopic tensile strength (left axis, blue bars) and microstructural uniformity standard deviation (right axis, red line) at varying WER contents. A distinct inflection point is observed at 12% WER content. Below this threshold, the tensile strength increases significantly with increasing WER, while the uniformity SD remains relatively low. Once the WER content exceeds 12%, the tensile strength growth slows down dramatically, accompanied by a sharp increase in

the uniformity SD, indicating that epoxy agglomeration (reflected by the uniformity SD) acts as a bottleneck limiting the further enhancement of macroscopic mechanical properties. In addition to tensile strength, a similar correlation exists between the complex modulus (G*) and microstructure. The growth of G* also significantly slows down when the WER content exceeds 12%, consistent with the deterioration of dispersion uniformity. Therefore, the microstructural parameters extracted from image analysis serve as reliable predictors for the performance thresholds of both mechanical strength and rheological properties.

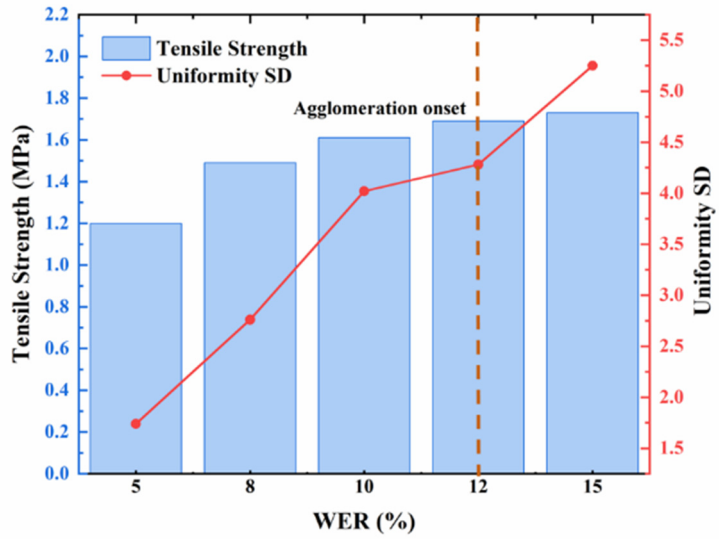


Figure 30. Pull-off strength vs. uniformity STD.

4. Conclusions

This study investigated different waterborne epoxy systems, and through systematic evaluation of their performance as well as their interaction with emulsified asphalt, the waterborne epoxy system with the best overall properties was identified. Subsequently, the performance of WER-modified emulsified asphalt was examined. Both macroscopic mechanical behavior and microscopic characterization were used to comprehensively evaluate the performance evolution of emulsified asphalt modified with WER and with the addition of SBR. The main conclusions are as follows:

(a) All three water-based curing agents mix well with water. The dissolution rate sequence is JT ≈ HM > KST. Among them, JT and HM water-based epoxy resins can be mixed well with emulsified asphalt, while KST has poor compatibility and a significant impact on particle size. Under an appropriate ratio, the bonding strength of the JT system is the best, and the coating film formation effect, curing reaction speed and volume stability of HM are all better than those of KST. Comprehensive evaluation shows that the performance of the JT water-based epoxy system is the best, and through the pull-out test, its optimal ratio is determined to be 1:0.6.

(b) The addition of WER can significantly enhance the bonding strength of emulsified asphalt. When the WER content is 5–10%, the bonding strength increases most significantly, and after exceeding 10%, the increase in bonding strength slows down. The addition of SBR can further improve the bonding strength on the basis of WER, with an increase range of 4–10%. The modified water-boiling test demonstrates that WER significantly enhances the adhesion between emulsified asphalt and aggregates, which suggests that the combination of WER and SBR could offer improved resistance to water damage under wet conditions. Rheological tests show that adding WER can significantly increase the complex modulus and storage modulus of WERAE.

(c) The novel image recognition algorithm successfully quantifies the dispersion of WER in the asphalt matrix. Quantitative correlation analysis reveals a critical trade-off point at a WER content of 12%. Below this threshold, the distribution uniformity standard deviation remains low, and the macroscopic bonding strength and complex modulus exhibit rapid growth. Once the WER content exceeds 12%, the uniformity standard deviation increases significantly ($p < 0.05$), indicating the onset of severe local agglomeration. This microstructural deterioration directly corresponds to the observed slowdown in macroscopic performance improvements. Therefore, to balance microstructural homogeneity and mechanical performance, the optimal WER content is recommended to be in the 10–12% range, with 12% identified as the critical upper limit. It should be noted that direct chemical bonding evidence was not experimentally characterized via FTIR in this study; discussions on the interfacial chemical mechanisms are primarily supported by existing literature.

5. Outlook

Future research will focus on the following key aspects to bridge the gap between the current findings and full-scale engineering applications.

First, to thoroughly assess the durability and full life-cycle performance of the WERAE system, the Pressure Aging Vessel (PAV) test will be systematically incorporated into the experimental program. Although the current work focused on fundamental mechanisms and fresh-state properties, considering that WERAE is predominantly used in preventive maintenance applications such as micro-surfacing and slurry seals, where short- to medium-term performance (3–5 years) is the primary concern, subsequent studies will couple PAV-accelerated aging with DSR rheological characterization and microstructural evolution analysis.

Second, the Multiple Stress Creep Recovery (MSCR) test, which is widely recognized as a robust indicator for evaluating the high-temperature elastic recovery and permanent deformation resistance of modified binders under repeated heavy traffic loads, was not included in this study due to experimental cycle constraints and the core focus on establishing quantitative relationships between microscopic dispersion parameters and linear viscoelastic properties. To address this limitation, future work will prioritize MSCR testing to systematically investigate the non-linear creep recovery characteristics of the WER/SBR composite-modified emulsified asphalt under high-stress loading conditions, thereby further validating its suitability for heavy-traffic pavement applications.

Third, it is recognized that the ultimate performance of asphalt mixtures is strongly governed by the characteristics of mineral fillers, despite the confirmed enhancements in binder bonding and rheological properties imparted by the WER microstructural network. As highlighted in a previous study [22], the mineral composition and particle morphology of fillers can significantly alter the viscoelastic behavior of asphalt mastic. Therefore, systematic investigations will be conducted to explore the compatibility and interfacial adsorption mechanisms between various mineral fillers (e.g., limestone powder and granite powder) and the WER-modified asphalt mastic. Together, these efforts will provide a more comprehensive understanding of the material's long-term service behavior and field performance, ultimately accelerating its reliable deployment in practical mixture design and pavement construction.

Author Contributions: The author's contributions to the paper are as follows: Research conception and design: W.Z., S.H. and J.O.; Data collection: Y.S. and J.O.; Result analysis and interpretation: W.Z., S.H., S.Z. and J.O.; Manuscript writing: Q.L., Y.S. and J.O. All authors have read and agreed to the published version of the manuscript.

Funding: The authors sincerely thank the Zhejiang Provincial Department of Transportation for the financial support provided under project 2025007, and the National Natural Science Foundation of China for the support under project 52568063.

Data Availability Statement: Data will be made available on request.

Conflicts of Interest: Authors Wei Zhang, Shi Hu, Shuai Zhang and Qin Liu were employed by the company Zhejiang Communications Investment Group Construction Management Co., Ltd. The remaining authors declare that the research was conducted in the absence of any commercial or financial relationships that could be construed as potential conflicts of interest.

References

1. He, L.; Hou, Y.; Yang, F. Study of the Properties of Waterborne Epoxy Resin Emulsified Asphalt and Its Modification Mechanism. *J. Mater. Civ. Eng.* **2023**, *35*, 04023145. [CrossRef]
2. Zhang, Y.J.; Wu, W.M.; Cao, H.S.; Zhao, L.D.; Zhang, Y.L.; Liu, B.Q.; Li, Y.; Cao, D.W. Investigation and evaluation of the emulsified asphalt with waterborne epoxy resin. *Key Eng. Mater.* **2020**, *842*, 337–345. [CrossRef]
3. Zhang, Q.; Xu, Y.H.; Wen, Z.G. Influence of water-borne epoxy resin content on performance of waterborne epoxy resin compound SBR modified emulsified asphalt for tack coat. *Constr. Build. Mater.* **2017**, *153*, 774–782. [CrossRef]
4. Lu, P.X.; Gong, M.H. Toughness Reinforcement Design of Grouting Materials for Semi-Flexible Pavements Through Water-Based Epoxy Resin and Emulsified Asphalt. *Coatings* **2025**, *15*, 493. [CrossRef]
5. Liu, X.; Wu, Z.; Min, Z.; Zhang, L. Investigation on the Preparation and Performances of Epoxy-Modified Asphalt Binder and Its Mixtures. *Materials* **2024**, *17*, 2539. [CrossRef] [PubMed]
6. Yang, F.; Yang, L.M.; Zhou, Q. Research on pavement performance of waterborne epoxy resin-modified emulsified asphalt binders and pothole repair materials. *Mater. Tehnol.* **2025**, *59*, 55–56. [CrossRef]
7. Li, P.; Ji, J.; Wang, Z.; Wu, Y.; Suo, Z.; Dong, Y.; Xu, M. Performance evaluation and equivalent conversion of waterborne epoxy resin emulsified asphalt based on different evaporation methods. *J. Clean. Prod.* **2022**, *353*, 131461. [CrossRef]
8. Feng, L.; Zhang, X.Y.; Sha, T.Y. A Rheological Study of the High-Temperature Properties of Fast-Melting SBS/Epoxy-Modified Asphalt Binders. *Polymers* **2025**, *17*, 581. [CrossRef] [PubMed]
9. He, G.; Lin, C.; Fang, G.; Lu, T.; Pan, Z.; Meng, Y. Study on the basic technical indicators and high-temperature rheological properties of SBR/WER modified emulsified asphalt waterproofing binder. *Constr. Build. Mater.* **2025**, *492*, 142923. [CrossRef]
10. Li, R.; Leng, Z.; Li, G.; Yang, B.; Lu, G. Effects of aging on rheological, chemical, and micromechanical properties of waterborne epoxy resin modified bitumen emulsion. *Int. J. Pavement Eng.* **2022**, *24*, 2077943. [CrossRef]
11. Yang, J.; Zhang, Z.; Fang, Y.; Luo, Y. Performance characterization of waterborne epoxy resin and styrene–butadiene rubber latex composite modified asphalt emulsion (WESAE). *Coatings* **2020**, *10*, 352. [CrossRef]
12. Huang, S.; Jin, F.; Chen, D.; Xiao, Q.; Ding, Q. Study on modification mechanism and performance of waterborne epoxy resin micro-surfacing. *Coatings* **2023**, *13*, 504. [CrossRef]
13. Fu, H.; Wang, C.; Niu, L.; Yang, G.; Liu, L. Composition optimisation and performance evaluation of waterborne epoxy resin emulsified asphalt tack coat binder for pavement. *Int. J. Pavement Eng.* **2021**, *23*, 4034–4048. [CrossRef]
14. Cong, P.; Tian, Y.; Liu, N.; Xu, P. Investigation of epoxy-resin-modified asphalt binder. *J. Appl. Polym. Sci.* **2016**, *133*, 43401. [CrossRef]
15. Han, S.; Yao, T.; Han, X.; Hongwei, Z.; Yang, X. Performance evaluation of waterborne epoxy resin modified hydrophobic emulsified asphalt micro-surfacing mixture. *Constr. Build. Mater.* **2020**, *249*, 118835. [CrossRef]
16. Li, R.; Chen, Y.Y.; Leng, Z.; Zhu, H.; Chen, Z. Application of Waterborne Epoxy Resin Modified Bitumen Emulsion as a Tack Coat Material. *J. Mater. Civ. Eng.* **2024**, *36*, 04024163. [CrossRef]
17. Ji, J.; Yao, H.; Zheng, W.; Suo, Z.; Xu, Y.; Han, S.; Xu, S.; You, Z. Preparation and Properties of Waterborne Epoxy-Modified Emulsified Asphalt Binder (WEMEAB). *J. Test. Eval.* **2020**, *48*, 3172–3187. [CrossRef]
18. Gu, Y.; Tang, B.; He, L.; Yang, F.; Wang, H.; Ling, J. Compatibility of cured phase-inversion waterborne epoxy resin emulsified asphalt. *Constr. Build. Mater.* **2019**, *229*, 116942. [CrossRef]
19. Cuadri, A.A.; Delgado-Sánchez, C.; Navarro, F.J.; Partal, P. Short-and long-term epoxy modification of bitumen: Modification kinetics, rheological properties, and microstructure. *Polymers* **2020**, *12*, 508. [CrossRef] [PubMed]
20. Wang, P.; Tian, X.; Zhang, R.; Zhen, S. Effect of waterborne epoxy resin on properties of modified emulsified asphalt and its microstructure. *J. Mater. Civ. Eng.* **2021**, *33*, 04021177. [CrossRef]
21. Ji, J.; Shi, Q.; Zhang, R.; Suo, Z.; Wang, J. Viscosity, mechanical properties and phase-separated morphology of waterborne epoxy asphalt. *Constr. Build. Mater.* **2022**, *334*, 127074. [CrossRef]
22. Lima, M.S.S.; Thives, L.P.; Haritonovs, V.; Gschösser, F. The Influence of Alternative Fillers on the Adhesive Properties of Mastics Fabricated with Red Mud. *Materials* **2020**, *13*, 484. [CrossRef] [PubMed]

23. Zhou, H.R.; Fang, X.J. Preparation and Properties of the Phase Inversion Emulsification of Epoxy Resin. *Adv. Mater. Res.* **2014**, *1021*, 7–10. [CrossRef]
24. Shree, R.; Naik, R.B.; Naik, R.S.; Gunasekaran, G. Effect of three structurally different epoxy resins on fire resistance, optical transparency, and physicomechanical properties of intumescent fire-retardant transparent coatings. *J. Coat. Technol. Res.* **2021**, *18*, 535–547. [CrossRef]
25. Marchfelder, C.; Pugstaller, R.; Wallner, G.M.; Brüggemann, O.; Aufray, M. Effect of epoxy structure on properties of waterborne coatings and electrical steel laminates. *Polymers* **2022**, *14*, 1556. [CrossRef] [PubMed]
26. Fazeli, M.; Liu, X.; Rudd, C. The effect of waterborne polyurethane coating on the mechanical properties of epoxy-based composite containing recycled carbon fibres. *Surf. Interfaces* **2022**, *29*, 101684. [CrossRef]
27. Li, R.; Leng, Z.; Zhang, Y.; Ma, X. Preparation and characterization of waterborne epoxy modified bitumen emulsion as a potential high-performance cold binder. *J. Clean. Prod.* **2019**, *235*, 1265–1275. [CrossRef]
28. Zhang, D.; Liu, Z.; Liang, S.; Zeng, Z. Low-temperature performance grading of asphalt binder through dynamic shear rheometer (DSR) testing: A case study in China. *Road Mater. Pavement Des.* **2025**, *27*, 2061–2087. [CrossRef]
29. Zeng, Z.; Underwood, B.S.; Castorena, C. Low-temperature performance grade characterisation of asphalt binder using the dynamic shear rheometer. *Int. J. Pavement Eng.* **2024**, *23*, 811–823.
30. Li, S.; Tan, Y.; Luo, W.; Xu, H.; Han, M.; Li, J.; Xiao, S. Novel Oil-Absorbing Organogel for Asphalt Pavement: VOC Reduction, Mechanical Properties, and Environmental and Economic Influence. *ACS Sustain. Chem. Eng.* **2026**, *14*, 6879–6892. [CrossRef]
31. Wang, W.; Duan, L.; Wang, Y. Fast Image Segmentation Using Two-Dimensional Otsu Based on Estimation of Distribution Algorithm. *J. Electr. Comput. Eng.* **2017**, *2017*, 1735176. [CrossRef]
32. Liu, Z.; Zhang, D.; Liu, H.; Xi, L.; Xu, S.; Liang, S. Development of high-fidelity digital aggregate data base for asphalt mixture through a novel generation algorithm and virtual sieving approach. *Powder Technol.* **2026**, *479*, 122549. [CrossRef]

Disclaimer/Publisher's Note: The statements, opinions and data contained in all publications are solely those of the individual author(s) and contributor(s) and not of MDPI and/or the editor(s). MDPI and/or the editor(s) disclaim responsibility for any injury to people or property resulting from any ideas, methods, instructions or products referred to in the content.